J. Am. Chem. Soc. **1996,** *118,* 6167−6184

Geometric Requirements for Hydrogen Abstractability and 1,4-Biradical Reactivity in the Norrish/Yang Type II Reaction: Studies Based on the Solid State Photochemistry and X-ray Crystallography of Medium-Sized Ring and Macrocyclic Diketones[†]

Anna D. Gudmundsdottir, Thillairaj J. Lewis, Leslie H. Randall,
John R. Scheffer,* Steven J. Rettig, James Trotter, and Chung-Hsi Wu

Contribution from the Department of Chemistry, University of British Columbia, 2036 Main Mall, Vancouver, Canada V6T 1Z1

Received October 10, 1995[⊗]

Abstract: The Norrish/Yang type II photochemistry of ten even-numbered cyclic diketones ranging in ring size from 10-membered to 26-membered has been studied in the crystalline state as well as in solution. In the solid state, the diketones undergo stereoselective cyclobutanol formation in which the *cis* or *trans* ring fusion stereochemistry of the photoproducts is governed by the conformation of the diketone present in the crystal as determined by X-ray crystallography. The reactive γ-hydrogen atoms are identified and the distance and angular parameters associated with their abstraction are derived from the crystallographic data. For the most part, the abstractions occur through boatlike rather than chairlike six-atom geometries, and the average value of **d**, the $C{=}O\cdots H$ abstraction distance, for 16 reactive γ-hydrogens was found to be 2.74 ± 0.04 Å; the average values of the angular parameters ω (the γ-hydrogen out-of-plane angle), Δ (the $C{=}O\cdots H_\gamma$ angle), and θ (the $C{-}H_\gamma\cdots O$ angle) are 53 ± 5°, 83 ± 4°, and 115 ± 2°, respectively. In a similar manner, the geometric parameters associated with the ring closure reactions of the intermediate 1,4-hydroxy biradicals were estimated from the crystallographic data. This indicates that both the pre-*cis* and pre-*trans* biradicals are poorly aligned for cleavage but are well oriented for closure, with radical separations of 3.1−3.2 Å. For four of the diketones, the solid state photoproduct ratios were found to be temperature dependent as a result of enantiotropic phase transitions. For two of the diketones, the high-temperature, metastable phases were characterized by solid state ^{13}C and ^{2}H NMR spectroscopy. Crystals of 1,14-cyclohexacosanedione were found to be dimorphic, and the conformation adopted by the macrocycle is very different in the two dimorphs. As a result, irradiation of one of the dimorphs leads to *cis*-cyclobutanol and photolysis of the other gives *trans*, a particularly clear demonstration of the effect of conformational polymorphism on solid state chemical reactivity. Overall, the solid state results indicate that the product distribution is determined by the relative rates of forward rather than reverse hydrogen atom transfer and that the biradicals react in a least-motion, conformation-specific manner. In solution, on the other hand, the photoreaction is ring size-dependent, resembling the solid state results for the 12- and 14-membered-ring diketones, and consisting mainly of type II elimination accompanied by reduced amounts of nonstereoselective cyclobutanol formation for the 16−26-membered-ring compounds. It is suggested that this ring size dependence stems from the relative conformational freedom of the intermediate 1,4-biradicals in the fluid medium—motions that are slow compared to closure for the 12- and 14-membered rings, but that permit alignment for biradical cleavage and alternative modes of closure in the “floppier” 16-membered and larger rings. The one exception to the above generalizations is 1,6-cyclodecanedione, which was found to be photochemically inert both in the solid state and solution despite having a crystal conformation favorable for type II photochemistry. Possible reasons for this behavior are presented and discussed.

Introduction

Crystals provide ideal environments for studying the effect of molecular structure on chemical reactivity.[1] Reactant structure can be determined in great detail through the use of X-ray crystallography and, because of crystal lattice forces that severely restrict molecular motion, this structural information can be used to model transition states and intermediates for reactions carried out in the solid state. The present paper describes the application of this so-called Crystal Structure−Reactivity Correlation Method to the photochemistry of a homologous series of medium-sized ring and macrocyclic diketones.[2]

Our interest in the macrocyclic diketone system was stimulated by a paper by Allinger *et al.* on the X-ray crystal and molecular structure of 1,10-cyclooctadecanedione (**1e**, Scheme 1).[3] This material crystallizes with C_{2h} molecular symmetry, and this conformation brings each ketone oxygen atom to within 2.78 Å of two neighboring γ-hydrogen atoms, a distance that,

---

[†] Based on the Ph.D. thesis of T. J. Lewis, the University of British Columbia, March, 1993.

[⊗] Abstract published in *Advance ACS Abstracts,* June 1, 1996.

(1) For a recent review of organic photochemistry in crystals and other organized media, see: *Photochemistry in Organized and Constrained Media*; Ramamurthy, V., Ed.; VCH Publishers: New York, 1991.

(2) Portions of this work have appeared in preliminary communication form: (a) Lewis, T. J.; Rettig, S. J.; Scheffer, J. R.; Trotter, J.; Wireko, F. *J. Am. Chem. Soc.* **1990**, *112*, 3679. (b) Lewis, T. J.; Rettig, S. J.; Scheffer, J. R.; Trotter, J. *J. Am. Chem. Soc.* **1991**, *113*, 8180. (c) Lewis, T. J.; Rettig, S. J.; Scheffer, J. R.; Trotter, J. *Mol. Cryst. Liq. Cryst.* **1992**, *219*, 17.

(3) Allinger, N. L.; Gorden, B. J.; Newton, M. G.; Lauritsen-Norskov, L.; Profeta, S., Jr. *Tetrahedron* **1982**, *38*, 2905.

S0002-7863(95)03420-2 CCC: $12.00

according to previous work from our laboratory,[4] should allow for facile Norrish type II hydrogen atom abstraction upon UV-irradiation of the crystals. 1,10-Cyclooctadecanedione (**1e**) belongs to a class of compounds known as the "diametric" diketones, defined as cyclic diketones in which the carbonyl groups are separated on each side by an equal number of methylene groups. Necessarily of even-numbered ring size, the smallest member of the homologous series is 1,3-cyclobutanedione, and the largest prepared so far is the 34-membered-ring compound, 1,18-cyclotetratriacontanedione. First prepared in the 1920s and 1930s by Ruzicka *et al*. in connection with their work on perfumery constituents,[5] most members of the series are beautifully crystalline, moderately high melting solids that are readily prepared (although often in low yield) by well-documented procedures.

Because it seemed likely that all members of the series with ring sizes ≥10 would have solid state conformations with abstractable γ-hydrogen atoms, we synthesized the diametric diketones ranging in ring size from 10- to 26-membered (**1a**−**i**, Scheme 1) and undertook an investigation of their solid state photochemistry. For reasons that will become clear later, we also prepared and photolyzed the non-diametric 16-membered-ring diketone **1j**. The primary goal of the work was to provide, through crystal structure−reactivity correlations, further information on the distance and angular requirements for intramolecular γ-hydrogen atom abstraction. Secondly, because the biradical intermediates formed by abstraction are immobilized in the crystal lattice in conformations similar to their ground state progenitors, such a study allows conclusions to be drawn regarding the effect of structure on 1,4-biradical partitioning. A particularly intriguing third goal of the project was to investigate the solid−solid phase transitions that have been reported[6] for some of the macrocyclic diketones and to determine their influence, if any, on the solid state photochemistry. A fourth goal of the study was to investigate the solution phase photochemistry of the macrocyclic diketones in order to make comparisons between their solid and solution state behavior. Although the solution phase photochemistry of several medium-sized and macrocyclic *mono*ketones has been studied quite thoroughly,[7−9] no previous investigation of the corresponding diametric diketones has been reported.

The solid state structure−reactivity correlation method requires a knowledge of the crystal and molecular structures of the diketones, and a fifth goal of the project was to obtain these through single-crystal X-ray diffraction analysis. This was successfully accomplished, and we anticipate that the results will be of considerable interest to those concerned with the conformational analysis of macrocyclic and medium-sized-ring compounds. Also included in the present paper are the results of molecular mechanics calculations designed to determine whether the shapes of the diketones in the solid state correspond to minimum energy conformations.

Results

Preparation of Starting Materials. Diketones **1a**−**i** were prepared according to published procedures (see supporting information for details). Only one new diketone, the nondiametric 1,8-cyclohexadecanedione (**1j**), was synthesized in the present study. This was prepared by a "mixed Blomquist" reaction involving treatment of a 1:1 mixture of suberyl chloride and sebacoyl chloride with triethylamine followed by hydrolysis and decarboxylation under basic conditions.[10] This procedure also gave diametric diketones **1c** and **1e,** from which diketone **1j** could be separated in 11% yield by column chromatography on silica gel.

An interesting byproduct, γ-pyrone derivative **3c**, was obtained in 21% yield during the preparation of diketone **1c** from suberyl chloride by the Blomquist procedure. A similar result was obtained when pimeloyl chloride was subjected to the Blomquist procedure. In this case, octahydroxanthone (**3b**) was obtained in 56% isolated yield, and only traces of diketone **1b** could be detected by gas chromatography. The structure of this material was established by comparing its spectroscopic and physical properties with those reported for the same compound prepared by catalytic hydrogenation of xanthone;[11] compound **3c** is apparently a new compound, but its spectra leave no doubt about its structure. The reaction is of limited synthetic utility, however, as attempts to isolate the γ-pyrones with 5- and 8-membered rings were unsuccessful. The mechanism by which pyrones **3b** and **3c** are produced is complex and need not be discussed in detail here other than to say that it may involve the formation and dimerization of the α-keto-ketene species **2b** and **2c**, respectively, followed by hydroxide ion-initiated conversion of the dimers to product (Scheme 1).[12]

Preparative Photochemical Studies in Solution and Characterization of the Photoproducts. In order to have a basis of comparison for the solid state studies, all ten diketones **1a**−**j** were first irradiated in solution and their photoproducts separated and identified. In every case except one, direct photolysis in hexane led to smooth γ-hydrogen abstraction and the formation of a mixture of the Yang reaction[13] products **4** and **5** as well as the type II elimination product **6** (Scheme 2). The lone exception was 1,6-cyclodecanedione (**1a**), which proved to be inert under all direct and sensitized photolysis conditions employed. In order to check whether this apparent lack of reactivity might be due to rapid and reversible hydrogen atom transfer, diketone **1a** was photolyzed in the good hydrogen bonding solvent *tert*-butyl alcohol. As Wagner has shown,[14] such solvents retard reverse hydrogen transfer through hydrogen bonding to the hydroxyl proton of the 1,4-hydroxy biradical intermediate, thus increasing the quantum yield of photoproduct formation. This can lead to the formation of new photoproducts,

---

[4] Scheffer, J. R. In *Organic Solid State Chemistry*; Desiraju, G. R., Ed.; Elsevier: Amsterdam, 1987; Chapter 1.

[5] (a) Ruzicka, L.; Brugger, N.; Seidel, C. F.; Schinz, H. *Helv. Chim. Acta* **1928**, *11*, 496. (b) Ruzicka, L.; Stoll, M.; Huyser, H. W.; Boekenoogen, H. A. *Helv. Chim. Acta* **1930**, *13*, 1152.

[6] Alvik, T.; Borgen, G.; Dale, J. *Acta Chem. Scand*. **1972**, *26*, 1805.

[7] Schulte-Elte, K. H.; Willhalm, B.; Thomas, A. F.; Stoll, M.; Ohloff, G. *Helv. Chim. Acta* **1971**, *54*, 1759.

[8] Burchill, P. J.; Kelso, A. G.; Power, A. J. *Aust. J. Chem*. **1976**, *29*, 2477.

[9] Matsui, K.; Mori, T.; Nozaki, H. *Bull. Chem. Soc. Jpn*. **1971**, *44*, 3440.

[10] (a) Blomquist, A. T.; Spencer, R. D. *J. Am. Chem. Soc*. **1948**, *70*, 30. (b) Blomquist, A. T.; Prager, J.; Wolinsky, J. *J. Am. Chem. Soc*. **1955**, *77*, 1804.

[11] Cordonnier, G.; Sliwa, H. *J. Hetereocycl. Chem*. **1978**, *24*, 111.

[12] Interestingly, treatment of adipyl chloride with triethylamine is reported to lead to a dimer of structure **i** (Baldwin, J. E. *J. Org. Chem*. **1963**, *28*, 3112), and treatment of this compound with aqueous sodium hydroxide was shown to lead to hydroxy-acid **ii**. On this basis, we tend to rule out a dimer analogous to **i** as being responsible for the formation of γ-pyrones **3b** and **3c** from suberyl and pimeloyl chloride, respectively. For a recent review on the subject of bisketenes and related compounds, see: Allen, A. D.; Ma, J.; McAllister, M. A.; Tidwell, T. T.; Zhao, D. *Acc. Chem. Res*. **1995**, *28*, 265.

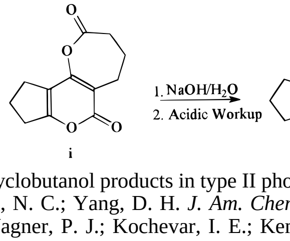

[13] Cyclobutanol products in type II photochemistry were first reported by: Yang, N. C.; Yang, D. H. *J. Am. Chem. Soc*. **1958**, *80*, 2913.

[14] Wagner, P. J.; Kochevar, I. E.; Kemppainen, A. E. *J. Am. Chem. Soc*. **1972**, *94*, 7489.

Scheme 1

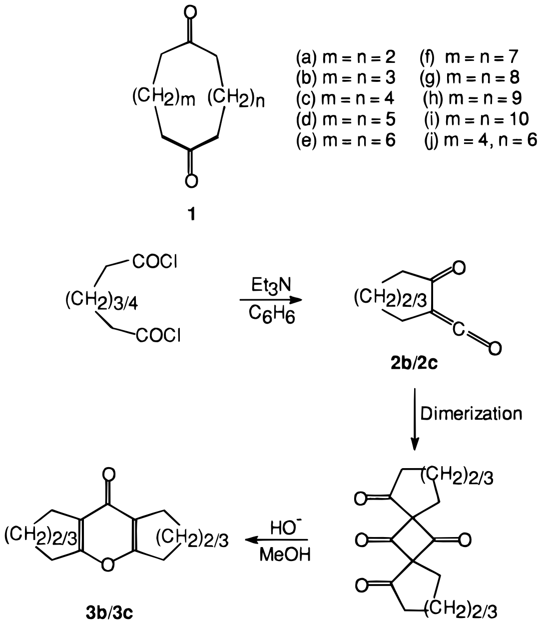

Scheme 2

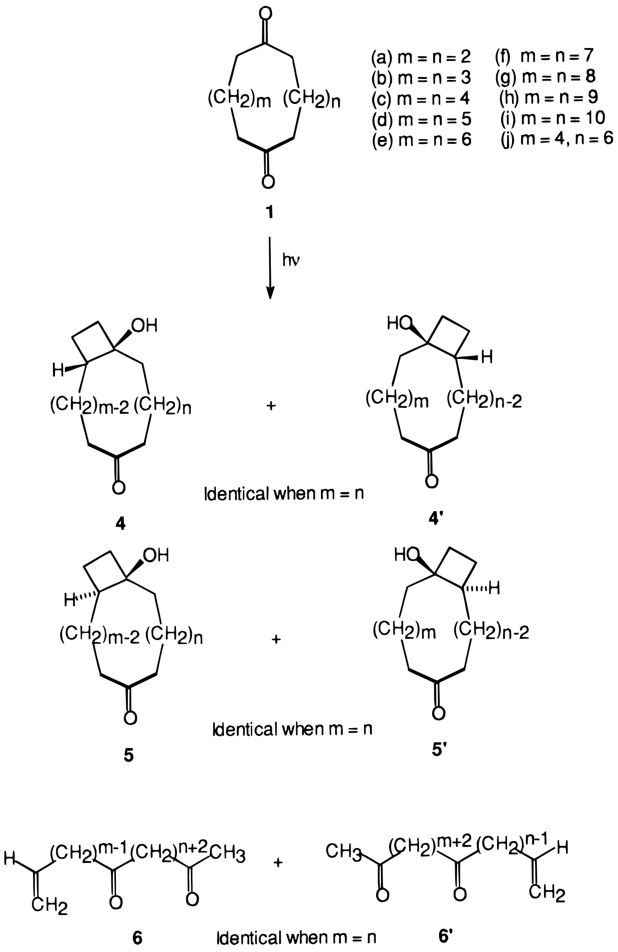

as Sauers and Huang have shown for cyclodecanone,[15] where irradiation in *tert*-butyl alcohol affords a γ-hydrogen abstraction-derived Yang reaction product in addition to the unusual ϵ-abstraction product that is formed when cyclodecanone is photolyzed in cyclohexane.[16] In the event, however, diketone **1a** remained photoinert in *tert*-butyl alcohol. Later in the paper, we shall discuss possible reasons for this interesting lack of photoproduct formation.

The photoproducts **4**, **5**, and **6** could all, with two exceptions, be isolated in pure form by column chromatography on silica gel. The exceptions were *trans*-cyclobutanol **5b**, which was not formed in the solid state or solution, and *cis*-cyclobutanol **4e**, which was characterized spectroscopically as part of a mixture as well as on the basis of its characteristic GC retention time. The ene-diones **6** could be differentiated readily from the other photoproducts by the appearance in their ^{1}H NMR spectra of methyl group signals as well as resonances characteristic of the $-CH{=}CH_2$ group (*ca.* δ 5–6 ppm).

In contrast, ^{1}H NMR was not very useful in determining the structure of the cyclobutanol photoproducts. These compounds were identified through their OH peaks in the IR and the presence in their mass spectra of an $M - 28$ peak due to the loss of ethylene *via* a $[2 + 2]$ cycloreversion of the 4-membered ring. The stereochemistry of the cyclobutanols was assigned primarily on the basis of an empirical correlation that was noted between their structure and the ^{13}C NMR chemical shift of the ring junction methine carbon atom. This carbon atom could be identified easily by the attached proton test, since it is the only one in the molecule that bears a single hydrogen atom. In the *cis*-cyclobutanols **4**, this carbon atom appears from 48.6 to 50.1 ppm, whereas in the trans series (**5**), it is found from 40.4 to 43.7 ppm. These assignments rest ultimately on the X-ray crystal structures of cyclobutanols **4d** (49.8 ppm) and **5f** (43.1 ppm).[17] A second empirical correlation that aided in the structural assignments was that involving the relative gas chromatographic retention times of the photoproducts. On a DB-17 fused silica capillary column (15 m × 0.25 mm, J & W Scientific), the elution order was invariably **6** followed by **5** followed by **4**.

The photoproduct structural assignments in the case of the nondiametric diketone **1j** presented a special challenge. This stems from the fact that, as shown in Scheme 2, there are four possible Yang cyclization products (**4j**, **4′j**, **5j**, and **5′j**) and two possible Norrish type II elimination products (**6j** and **6′j**). Two of these six photoproducts (**4j** and **4′j**) could be isolated in pure form by column chromatography, and their structures were ultimately proved by X-ray crystallography.[17] With a methine carbon chemical shift of 50.0 ppm in both cases, they conform to the chemical shift/structure correlation noted above. Photoproducts **5j** and **5′j** gave rise to a single peak on gas chromatography, and their relative proportions could therefore not be determined; their *total* contribution to the reaction mixture could, however, be measured. The same situation was observed in the case of the isomeric ene-diones **6j** and **6′j**.

Once the photoproducts had been fully characterized and identified, attention was directed to determining the solution phase (hexane) photoproduct distributions. Conversions were kept low in order to minimize possible secondary photoreactions of the products, which still contain potentially reactive carbonyl groups, and below 20%, the product ratios were found to be constant within experimental error. The photoproduct percentages, normalized to 100% and corrected for detector response, are collected in Table 1. It will be noted that the dimorphs of diketone **1i** afford identical photoproduct percentages in hexane, since all memory of previous crystal packing is lost in solution.

Sensitization, Quenching, and Quantum Yield Studies in Solution. In view of the likelihood that the solution phase results discussed above represent a combination of both singlet

---

[15] Sauers, R. R.; Huang, S.-Y. *Tetrahedron Lett.* **1990**, *31*, 5709.

[16] Bernard, M.; Yang, N. C. *Proc. Chem. Soc.* **1958**, 302.

[17] The crystallographic data for cyclobutanols **4d**, **5f**, **4j**, and **4′j** are compiled in Table 3.

Table 1. Solution Phase and Solid State Photoproduct Ratios[a]

	hexane			solid		
diketone	**4** (%)	**5** (%)	**6** (%)	**4** (%)	**5** (%)	**6** (%)
1a	no reaction			no reaction		
1b	84	00	16	**99**	00	01
1c	65	25	10	**58**	29	13
1d	22	35	43	**89**	10	01
1e	17	42	41	03	**84**	13
1f	10	23	67	**90**	04	06
1g	10	34	56	04	**91**	05
1h	15	27	58	**98**	01	01
1i needles	14	33	53	09	**91**	00
1i plates				**97**	03	00
	4/**4′**	**5**+**5′**	**6**+**6′**	**4**/**4′**	**5**+**5′**	**6**+**6′**
1j	13/13	35	39	**100**/00	00	00

[a] Photolyzed at 20 °C in Pyrex containers with the output from a 450-W Hanovia medium-pressure mercury lamp. Product ratios are normalized to 100%, corrected for GC detector response, and extrapolated to 0% conversion.

Table 2. Quantum Yields and Product Distribution in Photolysis of Diketone **1d**

entry	solvent	excited state	**4d** (%)	**5d** (%)	**6d** (%)	Φ_{total}
1	benzene	singlet + triplet[a]	18	30	52	0.104
2	benzene	singlet[b]	17	12	71	0.027
3	benzene	triplet[c]	18	36	46	0.077
4	*tert*-butyl alcohol	singlet + triplet[a]	21	27	52	0.148

[a] Direct irradiation in the absence of quencher. [b] Run in the presence of 7 M 2,3-dimethyl-1,3-butadiene. [c] Calculated from data in entries 1 and 2.

and triplet reactivity,[18] we thought it important to establish the fraction of total reaction coming from each excited state as well as the characteristic product distribution from each. The 16-membered-ring diketone **1d** was selected as a representative example on the basis of the excellent GC separation of its photoproducts.

Using standard techniques that are summarized in the Experimental Section, quantum yields for photoproduct formation were determined for diketone **1d** in benzene and *tert*-butyl alcohol (Table 2). Benzene was used as a non-hydrogen bonding solvent instead of hexane for solubility reasons in the quenching runs. We note that the product distribution from direct irradiation in benzene is slightly different from that observed in hexane. Table 2 also includes the product distribution and quantum yield for the pure singlet reaction conducted in the presence of a high concentration of the triplet quencher, 2,3-dimethyl-1,3-butadiene. A plot of the photoproduct ratios *versus* quencher concentration (not shown) levels off at approximately 5 M, and we assume that no triplet reactivity remains at or beyond this point.

The results indicate that the total quantum yield in *tert*-butyl alcohol, while approximately 42% higher than that in benzene, is still significantly less than unity, a finding that is consistent with most previous work on the type II photochemistry of aliphatic ketones.[18] Interestingly, in the case of cyclodecanone[15] and cyclododecanone,[8] the overall type II quantum efficiency actually *decreases* somewhat in going from hydrocarbon to hydroxylic solvents. It is also worth noting that the product distribution is not very solvent dependent in the case of diketone **1d**. In benzene, approximately 26% of the overall reaction upon direct irradiation occurs through the singlet state assuming that there is no quenching of this state by the diene. We attempted to check this by determining the quantum yield for the acetone-sensitized triplet process, but unlike Fleming and Long, who used acetone to sensitize the type II reaction of *cis*-2-propyl-4-*tert*-butylcyclohexanone,[19] we were unable to obtain reliable data. As is generally the case with aliphatic ketones,[20,21] we find that the cyclization to cleavage ratio for diketone **1d** is greater from the triplet state than from the singlet.

Photochemical Studies in the Solid State. The solid state irradiations were carried out by crushing the crystals between two Pyrex microscope slides, sealing the “sandwiches” under nitrogen in polyethylene bags, and photolyzing the resulting assemblies at room temperature with the output from a 450-W Hanovia medium pressure mercury lamp. In order to determine whether the photoproduct distribution was sensitive to surface phenomena or defects brought about by crushing, parallel photochemical studies on large, carefully grown single crystals were also performed. Very little difference between the two methods could be detected.

The diketones reacted much more selectively in the crystalline state than in solution. By far the major constituents of the solid state reaction mixtures were the cyclization photoproducts **4** and **5**, and depending on ring size, one of these was generally formed in much higher yield than the other. As was the case in solution, 1,6-cyclodecanedione proved to be completely unreactive. For the other diketones, crystal softening became apparent at conversions of 10% or more, and the product distributions became more solution-like. The photoproduct percentages were therefore determined as a function of conversion and extrapolated to 0%, and these data, corrected for detector response, are compiled in Table 1.

Crystallographic Studies. As mentioned in the introduction section, the crystal and molecular structure of the 18-membered-ring diketone **1e** was known when we began this work.[3] In addition, there was a 1933 report of an X-ray diffraction study of the 24-membered-ring diketone **1h** which concluded that this compound crystallizes in a long, thin unit cell.[22] Mention has also been made in the literature of the crystal structure of the 10-membered-ring diketone **1a**,[23] but as far as we are aware, the details have never been published. Therefore, at the same time as the photochemical work described above was being carried out, the crystal and molecular structures of diketones **1a**, **1c**, **1d**, **1f**−**1h**, **1i** (two polymorphs), and **1j** (nine structures in all) were successfully determined. Table 3 summarizes the crystallographic data, and Figure 1 gives CHARON drawings for each of the diketones studied; also included in Table 3 are crystallographic data for cyclobutanols **4d**, **4j**, **4′j**, and **5f**. Greater detail on the crystal structure determinations is provided in the Experimental Section and the supporting information.

In one case, that of the 12-membered-ring diketone **1b**, the crystal structure could not be determined; the crystals were twinned, and data collected with a cut, apparently untwinned fragment gave a structure with extensive disorder, which could not be modeled satisfactorily. In this instance, therefore, the minimum energy conformation was identified by a molecular mechanics calculation, and the conformational drawing shown in Figure 1b is based on the MM2 results. Similarly, the data in later tables that pertain to diketone **1b** are MM2-based rather than crystallographically-derived. The justification for assuming that this conformer is, in fact, the conformer present in the

---

(18) Wagner, P. J. *Acc. Chem. Res.* **1972**, *4*, 168.

(19) Fleming, I.; Long, W. E. *J. Chem. Soc., Perkin Trans. 2* **1976**, 14.

(20) (a) Coulson, D. R.; Yang, N. C. *J. Am. Chem. Soc.* **1966**, *88*, 4511. (b) Yang, N. C.; Elliot, S. P. *J. Am. Chem. Soc.* **1969**, *91*, 7550.

(21) Fleming, I.; Kemp-Jones, A. V.; Long, W. E.; Thomas, E. J. *J. Chem. Soc., Perkin Trans. 2* **1976**, 7.

(22) Müller, A. *Helv. Chim. Acta* **1933**, *16*, 155. Cell constants: $a = 9.91$ Å, $b = 8.13$ Å, $c = 30.79$ Å, $\beta = 68.5°$.

(23) Germain, G., personal communication as reported by: Dunitz, J. D. In *Perspectives in Structural Chemistry*; Dunitz, J. D., Ibers, J. A., Eds.; Wiley: New York, 1968; Vol. 2, p 495.

Table 3. Crystallographic Data[a]

compd	**1a**	**1c**	**1d**	**1f**	**1g**	**1h**	**1i (n)**	**1i (pl)**	**1j**	**4d**	**4j**	**4′j**	**5f**
formula	$C_{10}H_{16}O_2$	$C_{14}H_{24}O_2$	$C_{16}H_{28}O_2$	$C_{20}H_{36}O_2$	$C_{22}H_{40}O_2$	$C_{24}H_{44}O_2$	$C_{26}H_{48}O_2$	$C_{26}H_{48}O_2$	$C_{16}H_{28}O_2$	$C_{16}H_{28}O_2$	$C_{16}H_{28}O_2$	$C_{16}H_{28}O_2$	$C_{20}H_{36}O_2$
fw	168.24	224.34	252.40	308.50	336.56	364.61	392.66	392.66	252.40	252.40	252.40	252.40	308.50
color, habit	colorless, prism	colorless, prism	colorless, prism	colorless, plate	colorless, prism	colorless, plate	colorless, plate	colorless, prism	colorless, irreg	colorless, prism	colorless, prism	colorless, plate	colorless, prism
no., 2θ range (deg) for cell detrm	25, 35.4−43.3	25, 20.0−33.2	25, 39.7−52.5	25, 57.1−84.1	25, 75.2−79.9	25, 32.8−38.8	25, 25.4−38.5	25, 35.4−42.1	25, 101.7−114.3	25, 13.7−23.7	25, 75.1−91.1	25, 55.7−85.0	25, 20.6−25.1
crystal system	monoclinic	orthorhombic	triclinic	triclinic	monoclinic	monoclinic	monoclinic	monoclinic	monoclinic	triclinic	triclinic	monoclinic	triclinic
space group	$P2_1/n$	$Cmca$	$P\bar{1}$	$P\bar{1}$	$P2_1/c$	$P2_1/a$	$P2_1/c$	$P2_1/n$	$C2/c$	$P\bar{1}$	$P\bar{1}$	$P2_1/n$	$P\bar{1}$
a, Å	7.158(5)	16.624(3)	9.866(1)	11.8853(9)	15.408(1)	9.916(4)	8.107(2)	5.541(2)	19.539(1)	9.784(2)	9.1859(6)	9.3267(8)	9.607(2)
b, Å	5.449(4)	8.330(2)	14.923(2)	15.709(1)	5.508(1)	8.126(4)	5.526(1)	28.327(2)	8.0133(8)	9.885(3)	11.4458(9)	9.801(1)	12.034(2)
c, Å	11.61(1)	10.034(3)	5.453(1)	5.4613(6)	24.696(1)	28.625(2)	28.724(3)	8.005(2)	9.9005(6)	9.580(3)	8.2045(9)	16.7840(9)	9.578(2)
α, deg	90	90	95.03(2)	94.796(8)	90	90	90	90	90	116.59(2)	98.384(8)	90	95.78(2)
β, deg	95.99(8)	90	90.42(2)	95.397(8)	99.662(5)	92.29(1)	97.98(1)	98.89(3)	98.628(6)	109.88(2)	116.028(6)	101.351(6)	106.96(2)
γ, deg	90	90	75.38(1)	106.310(6)	90	90	90	90	90	95.91(2)	89.640(7)	90	68.82(2)
V, Å^3	450.6(6)	1389.4(5)	773.8(2)	967.8(2)	2066.0(4)	2305(1)	1254.3(7)	1241.3(6)	1532.6(2)	742(1)	765.2(1)	1504.2(2)	987.5(4)
Z	2	4	2	2	4	4	2	2	4	2	2	4	2
ρ_{calc}, g/cm^3	1.24	1.07	1.08	1.06	1.08	1.05	1.04	1.05	1.09	1.13	1.10	1.11	1.04
F(000)	184	496	280	344	752	816	440	440	560	280	280	560	344
radiation	Mo	Mo	Cu	Cu	Cu	Mo	Mo	Mo	Cu	Mo	Cu	Cu	Mo
μ, cm^{-1}	0.79	0.65	5.04	4.74	4.77	0.60	0.59	0.59	5.09	0.67	5.10	5.19	0.60
crystal size, mm	0.35×0.40×0.40	0.20×0.35×0.45	0.15×0.15×0.20	0.13×0.30×0.35	0.35×0.35×0.45	0.20×0.40×0.45	0.08×0.35×0.38	0.30×0.45×0.45	0.30×0.35×0.40	0.25×0.30×0.40	0.12×0.15×0.25	0.04×0.25×0.40	0.15×0.25×0.35
transmission factors	0.81−1.00	0.82−1.00		0.91−1.00	0.90−1.00	0.77−1.00	0.85−1.00	0.79−1.00	0.86−1.00	0.95−1.00	0.91−1.00	0.91−1.00	0.92−1.00
scan type	$\omega-2\theta$	$\omega-2\theta$	$\omega-2\theta$	$\omega-2\theta$	$\omega-2\theta$	ω	ω	ω	$\omega-2\theta$	$\omega-2\theta$	$\omega-2\theta$	$\omega-2\theta$	$\omega-2\theta$
scan range, ω°	1.15 + 0.35tanθ	1.15 + 0.35tanθ	1.10 + 0.30tanθ	1.20 + 0.20tanθ	1.30 + 0.30tanθ	1.10 + 0.35tanθ	0.95 + 0.35tanθ	1.20 + 0.35tanθ	1.20 + 0.35tanθ	1.50 + 0.35tanθ	1.05 + 0.20tanθ	1.05 + 0.20tanθ	1.21 + 0.35tanθ
scan rate, deg min^{-1}	16 (8 rescans)	32 (8 rescans)	32 (8 rescans)	32 (8 rescans)	16 (8 rescans)	32 (8 rescans)	16 (8 rescans)	32 (8 rescans)	32 (8 rescans)	32 (8 rescans)	32 (8 rescans)	16 (8 rescans)	32 (8 rescans)
data collected	$+h,+k,\pm l$	$+h,+k,+l$	$+h,\pm k,\pm l$	$+h,\pm k,\pm l$	$+h,+k,\pm l$	$+h,+k,\pm l$	$+h,+k,\pm l$	$+h,+k,\pm l$	$+h,+k,\pm l$	$+h,\pm k,\pm l$	$+h,\pm k,\pm l$	$+h,+k,\pm l$	$+h,\pm k,\pm l$
2θ_{max}, deg	65	50	150	155	155	55	55	60	155	60	155	155	55
crystal. decay, %	7.1	negligible	negligible	negligible	negligible	negligible	negligible	negligible	negligible	negligible	negligible	negligible	negligible
total no. of reflcns	1904	625	3425	4431	4380	5996	3457	4096	1792	4569	3329	3460	4801
no. of nique reflcns	1783	625	3074	3949	4226	5676	3393	3709	1744	4337	3119	3252	4532
R_{merge}	0.023		0.025	0.016	0.016	0.023	0.031	0.016	0.029	0.016	0.011	0.017	0.035
p factor[a]	0.02	0.025	0.05	0.03	0.05	0.025	0.025	0.03	0.005	0.05	0.01	0.01	0.02
no. with $I \geq 3\sigma(I)$	970	328	1854	2608	2821	2067	1404	1899	1392	2049	2315	1831	1610
no. of variables	88	41	276	344	378	236	128	223	139	276	168	168	207
R	0.034	0.073	0.036	0.034	0.047	0.036	0.037	0.035	0.030	0.038	0.039	0.036	0.046
R_w	0.038	0.089	0.049	0.045	0.063	0.045	0.043	0.043	0.039	0.045	0.049	0.039	0.050
gof	1.67	3.97	1.33	1.77	2.41	1.83	1.73	1.67	3.59	1.79	2.80	1.98	2.18
H atom treatment	refined	calculated	refined	refined	refined	calculated	calculated	refined	refined	refined	O−H refined C−H calcd	O−H refined C−H calcd	O−H refined C−H calcd
extinction coeff	$5.17(6) \times 10^{-5}$	$3.3(1) \times 10^{-5}$		$2.60(7) \times 10^{-5}$	$3.54(9) \times 10^{-5}$	$9.1(2) \times 10^{-7}$	$1.8(1) \times 10^{-6}$		$2.24(7) \times 10^{-5}$	$1.0(1) \times 10^{-6}$	$1.25(8) \times 10^{-5}$	$2.5(1) \times 10^{-6}$	
max Δ/σ (final cycle)	0.0003	0.0001	0.01	0.02	0.02	0.04	0.002	0.005	0.007	0.002	0.05	0.03	0.003
residual density, e/Å^3	−0.10 to 0.15	−0.15 to 0.24	−0.19 to 0.12	−0.11 to 0.12	−0.14 to 0.19	−0.09 to 0.11	−0.11 to 0.12	−0.12 to 0.14	−0.08 to 0.10	−0.12 to 0.15	−0.11 to 0.12	−0.11 to 0.12	−0.11 to 0.18

[a] Temperature 294 K, Rigaku AFC6S diffractometer, Mo Kα ($\lambda = 0.71069$ Å) or Cu Kα ($\lambda = 1.54178$ Å) radiation, graphite monochromator, takeoff angle 6.0°, aperture 6.0 × 6.0 mm at a distance of 285 mm from the crystal, stationary background counts at each end of the scan (scan/background time ratio 2:1), $\sigma^2(F^2) = [S^2(C + 4B) + (pF_o^2)^2]/Lp^2$ (S = scan rate, C = scan count, B = normalized background count), function minimized $\sum w(|F_o| - |F_c|)^2$ where $w = 4F_o^2/\sigma^2(F_o^2)$, $R = \sum||F_o| - |F_c||/\sum|F_o|$, $R_w = (\sum w(|F_o| - |F_c|)^2/\sum w|F_o|^2)^{1/2}$, and gof $= [\sum w(|F_o| - |F_c|)^2/(m-n)]^{1/2}$. Values given for R, R_w, and gof are based on those reflections with $I \geq 3\sigma(I)$.

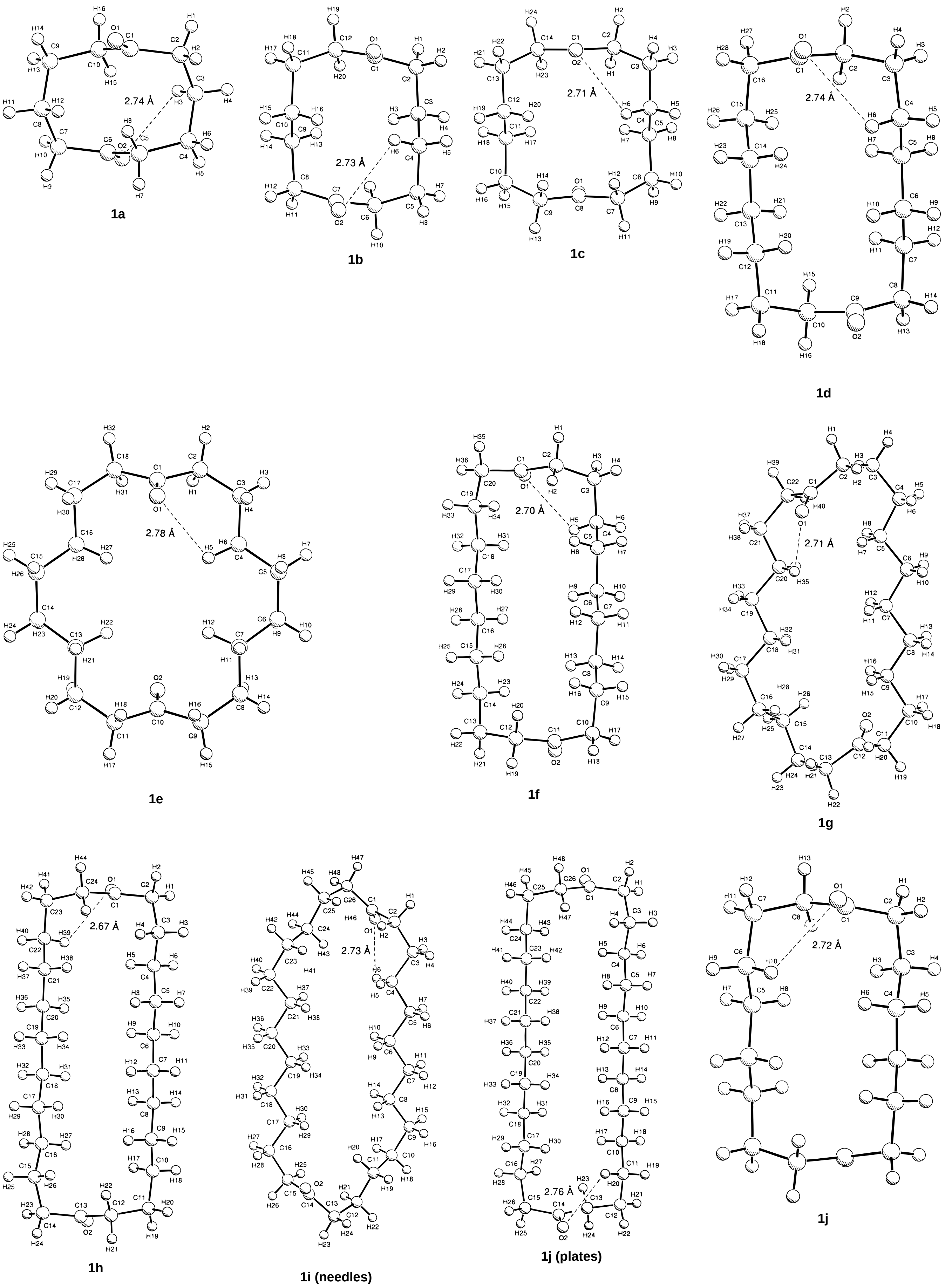

1a **1b** **1c** **1d** **1e** **1f** **1g** **1h** **1i (needles)** **1j (plates)** **1j**

Figure 1. Solid state conformations of diketones **1a**−**1j**. Closest γ-hydrogen atom contacts are shown by the dotted lines.

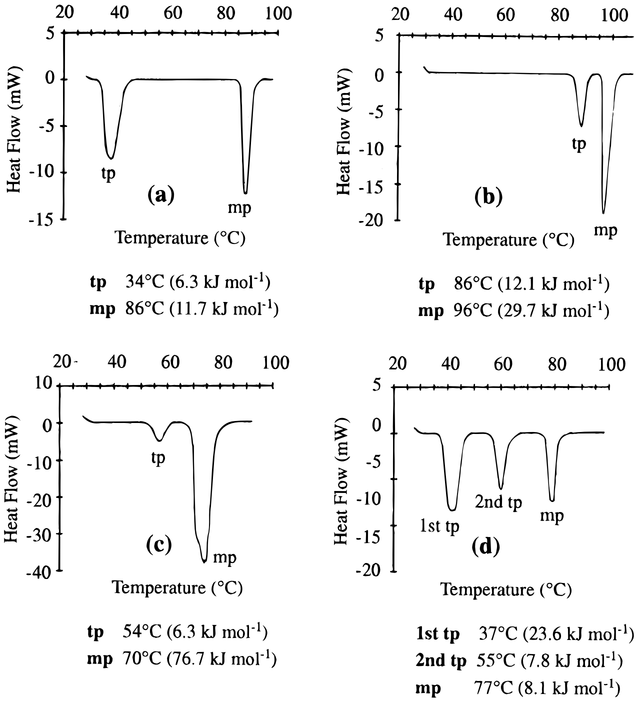

tp 34°C (6.3 kJ mol^{-1})
mp 86°C (11.7 kJ mol^{-1})

tp 86°C (12.1 kJ mol^{-1})
mp 96°C (29.7 kJ mol^{-1})

tp 54°C (6.3 kJ mol^{-1})
mp 70°C (76.7 kJ mol^{-1})

1st tp 37°C (23.6 kJ mol^{-1})
2nd tp 55°C (7.8 kJ mol^{-1})
mp 77°C (8.1 kJ mol^{-1})

Figure 2. Differential scanning calorimetry thermograms of (a) diketone **1d**, (b) diketone **1e**, (c) diketone **1i** (plate dimorph), and (d) diketone **1j**. Phase transition temperatures (°C) and the corresponding heats of transition (kJ mol^{-1}) are included.

crystalline state will be presented later in the paper along with more details on the molecular mechanics calculations.

Temperature Dependence of the Solid State Photochemical Results. One of the goals of our work was to investigate the influence that the sub-melting point phase transitions reported by Dale *et al.* for the 16- and 18-membered-ring diketones **1d** and **1e** have on the solid state photoproduct ratios. Dale and co-workers observed that diketone **1d** undergoes a solid−solid phase transition at 28 °C, well below its melting point of 78 °C, and that diketone **1e** exhibits a similar phase change at 86 °C before finally melting at 98 °C.[6] We verified these phase transitions by differential scanning calorimetry, the only difference between our results and Dale's being that we find a somewhat higher temperature transition point (34 °C) for the 16-membered-ring diketone **1d**. Figure 2 shows the DSC traces for diketones **1d** and **1e** along with the associated enthalpy changes. We also checked the DSC behavior of the other diketones and found that the plate-like crystal modification of the 26-membered-ring diketone **1i** undergoes a weak solid−solid phase transition at 54 °C, finally melting at 70 °C, and that the nondiametric diketone **1j** exhibits *two* endothermic phase transitions at 37 and 55 °C before melting at 77 °C. The DSC traces and ΔH values for these two compounds are included in Figure 2.

The solid−solid phase transition in the case of the plate dimorph of diketone **1i** proved to be irreversible, whereas the others were reversible. When slowly and carefully recrystallized from ethyl acetate−petroleum ether mixtures at room temperature, diketone **1i** deposited clear plates. When the plates were heated to temperatures between 54 and 70 °C they became polycrystalline and opaque, and after cooling to room temperature these so-called annealed crystals showed no sub-melting point phase transition and simply melted at 70 °C. Seeding of saturated solutions of diketone **1i** with the annealed crystals caused deposition of the needle dimorph of this compound. The crystal structure of each dimorph was successfully determined, and the results are shown in Figure 1. The needle and plate dimorphs of diketone **1i** are examples of conformational polymorphs—polymorphic crystal modifications that differ not only in packing arrangement but also in the conformation of the constituent molecules as well.[24]

Table 4. Photoproduct Percentages as a Function of Crystal Modification and Temperature for Diketone **1i**

entry	T (°C)	medium	**4i** (%)	**5i** (%)	**6i** (%)
1	0	plates	99	01	00
2	20	plates	97	03	00
3	40	plates	96	04	00
4	60	plates	19	81	00
5	65	plates	20	76	04
6	20	annealed plates	09	91	00
7	0	needles	07	93	00
8	20	needles	09	91	00
9	40	needles	11	89	00
10	60	needles	18	82	00
11	65	needles	17	83	00
12	20	solution (hexane)	14	33	53

The conclusion from these experiments is that the plate dimorph is metastable and is converted into the stable needle dimorph of diketone **1i** above 54 °C. Support for this view comes from the fact that the DSC trace, the ^{13}C CPMAS solid state NMR spectrum, the powder diffraction pattern, and the FTIR spectrum of the annealed plates are identical with those of the X-ray quality needles grown by recrystallization and quite different from those of the "virgin" plates. The product percentages obtained by photolysis of the virgin plates, the annealed plates, and the needles as a function of temperature also support this conclusion. Table 4 summarizes the results. As can be seen, the photochemical behavior of the annealed plates is essentially identical to that of the needles at the same temperature. Interestingly, the reaction selectivity decreases with increasing temperature below the melting point, but never reaches the distribution characteristic of the isotropic fluid state. Evidently, even at 65 °C, the reaction cavity maintains its basic anisotropic structure.

The temperature-dependent solid state photochemistry of diketone **1i** is very similar in principle to the results obtained by Cohen *et al.* for *trans*-cinnamic acid.[25] Like diketone **1i**, *trans*-cinnamic acid is dimorphic, having a metastable β-form that is transformed into a more stable α-form upon heating to approximately 50 °C, and because the dimorphs lead to different photodimers, the solid state photochemistry of the β-form changes as the transition temperature is traversed.

The behavior of diketones **1d**, **1e**, and **1j** was found to be quite different from that of diketone **1i**. In these cases, when the virgin crystals obtained by recrystallization from solution were heated above the transition point but below the melting point, the crystals became polycrystalline and opaque (as in the case of diketone **1i**), but upon cooling, the annealed crystals proved to be indistinguishable from the virgin samples by DSC. In other words, the higher temperature phases are metastable for these compounds and revert fairly rapidly to their original crystal modifications upon cooling. In order to characterize the high-temperature solid phases in more detail, variable-temperature ^{13}C CPMAS and wide-line ^{2}H solid state NMR studies were carried out for diketones **1d** and **1e**. The results of these studies are described below.

Figure 3 shows the ^{13}C CPMAS NMR spectra of the 16-membered-ring diketone **1d** at 27 °C (below the transition temperature) and at 37 °C (above the the transition temperature).

---

(24) Bernstein, J. In *Organic Solid State Chemistry*; Desiraju, G. R., Ed.; Elsevier: Amsterdam, 1987; Chapter 13, pp 471−518.

(25) Cohen, M. D.; Schmidt, G. M. J.; Sonntag, F. I. *J. Chem. Soc.* **1964**, 2000.

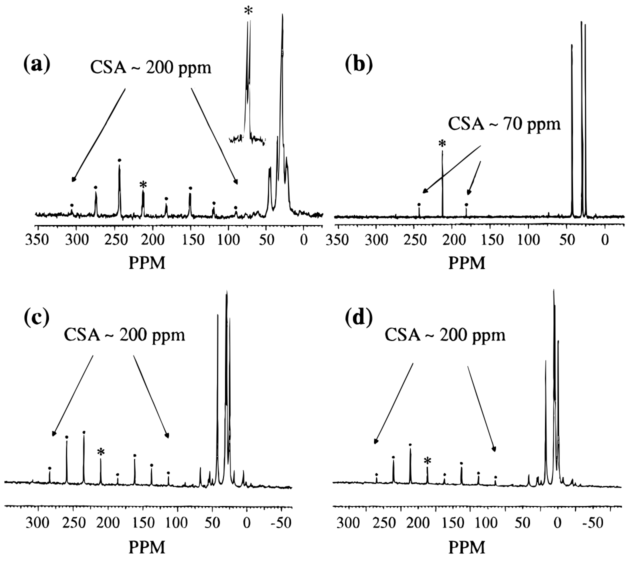

Figure 3. ^{13}CPMAS NMR spectra of diketone **1d** at (a) 27 and (b) 37 °C; diketone **1e** at (c) 27 and (d) 92 °C. The isotropic signals are indicated by an asterisk and the spinning side bands by a dot. The insert in (a) shows more clearly the splitting of the carbonyl carbon signal due to the lack of molecular symmetry.

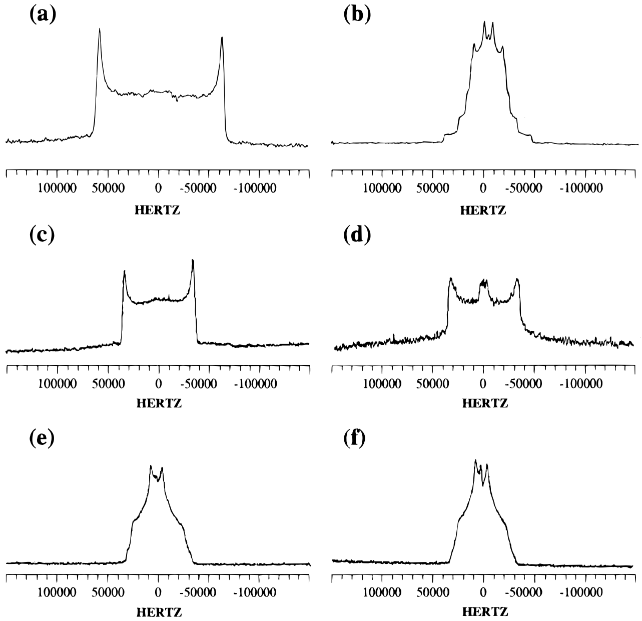

Figure 4. ^{2}H solid state NMR spectra of (a) diketone **1d** at 27 °C (below transition point), (b) **1d** at 37 °C (above transition point), (c) diketone **1e** at 47 °C, (d) **1e** at 67 °C, (e) **1e** at 77 °C (all below transition point), and (f) **1e** at 87 °C (above transition point).

Table 5. Photoproduct Percentages as a Function of Temperature for Diketone **1d**

	solid			hexane		
T (°C)	**4d** (%)	**5d** (%)	**6d** (%)	**4d** (%)	**5d** (%)	**6d** (%)
0	89	08	03			
10	90	07	03			
20	89	10	01	22	35	43
30	47	16	37	21	32	47
40	17	20	63	19	30	51
60	20	21	59	18	28	54
20 (annealed)	86	10	04			

Associated with the isotropic chemical shift of the carbonyl carbon in each case (indicated by an asterisk) is a series of spinning side bands indicated by dots. In rigid systems, where molecular motion is restricted, these side bands extend over a wide range of frequencies owing to the random distribution of the carbonyl group over all possible orientations in the polycrystalline sample (chemical shift anisotropy),[26] and this is what we see in Figure 3a. Note also that the carbonyl carbon resonances are doubled in the lower temperature spectrum owing to the lack of symmetry in the crystal conformation (see Figure 1d). The methylene carbons are also nonequivalent, and this is most clearly seen in the signals due to the carbons adjacent to the carbonyl groups. At 37 °C, the doubling of the carbonyl and methylene carbons disappears and the chemical shifts in the spectrum closely resemble those in the the fluid phase spectrum. The reduced but nevertheless significant (~70 ppm) anisotropy of the carbonyl chemical shift indicates that full isotropic motion has not been reached at this temperature, although the symmetry of the molecule has increased.

Also included in Figure 3 are the analogous ^{13}C CPMAS NMR spectra of the 18-membered-ring diketone **1e**, both below (27 °C) and above (92 °C) its solid solid phase transition point (86 °C). In this case there is no difference between the two spectra. The carbonyl carbon resonance is a singlet in both cases, which is consistent with the C_{2h} molecular symmetry present in the crystal (see Figure 1e). In addition, the spinning side band pattern is similar in both spectra, indicating that even at 92 °C, there is very little motion of the carbonyl group in the metastable solid phase. From this result we may tentatively conclude that the phase change in this compound is associated primarily with methylene chain reorientation.

In order to investigate the various solid phases of diketones **1d** and **1e** in greater detail, both compounds were fully deuterated in the α-position and studied by variable-temperature solid state ^{2}H NMR spectroscopy. Figure 4a shows the spectrum of diketone **1d**-d_8 at 27 °C (below the transition point), and the spectrum of the same sample at 37 °C (above the transition point) is given in Figure 4b. The deuterium spectra of diketone **1e**-d_8 at 47, 67, 77, and 87 °C are shown in Figures 4c−4f; only the final temperature lies above the transition point of 86 °C for this compound.

The observation of classic Pake powder patterns covering >100 kHz for diketone **1d** at 27 °C (Figure 4a) and diketone **1e** at 47 °C (Figure 4c) establishes that the C−D bonds in both diketones are conformationally fixed at these temperatures.[26] However, at higher temperatures the spectra become narrower and more complex, indicating that conformational motion of the CD_2 groups is occurring. In the case of the 18-membered-ring diketone **1e**, there is a significant change in the ^{2}H spectrum well below the phase transition temperature determined by differential scanning calorimetry, indicating the occurrence of large-amplitude rotational motions. Such is not the case for the 16-membered-ring diketone, and the spectra in this case are suggestive of an "inside-out" motion of the carbonyl groups correlated with the rotations of the CH_2 groups.

With the NMR results in hand, we next turned to a study of the solid state photochemistry of diketones **1d**, **1e**, and **1j** as a function of temperature. The results of these experiments are summarized in Tables 5−7. As can be seen, as the transition point is traversed in each case, there is a dramatic change in the photoproduct percentages in the direction of the distribution characteristic of the isotropic fluid phase at the same temperature. There are, however, small but significant differences between the results obtained in solution and in the high-temperature, metastable phases. In the case of diketone **1d**, for example, there is slightly more type II cleavage at 40 °C in the metastable solid state (63%) than in solution (51%). Conversely,

---

[26] Fyfe, C. A. *Solid State NMR for Chemists*; C.F.C. Press: Guelph, Canada, 1983.

Table 6. Photoproduct Percentages as a Function of Temperature for Diketone **1e**

	solid			hexane		
T (°C)	**4e** (%)	**5e** (%)	**6e** (%)	**4e** (%)	**5e** (%)	**6e** (%)
20	03	84	13	17	42	41
30	03	82	15	24	38	38
40	03	81	16	23	36	41
60	04	79	17	23	32	45
80	06	75	19	22	31	47
90	13	49	38	21	30	49
20 (annealed)	03	81	16			

Table 7. Photoproduct Percentages as a Function of Temperature for Diketone **1j**

	solid			hexane		
T (°C)	**4j**/**4j′** (%)	**5j**+**5j′** (%)	**6j**+**6j′** (%)	**4j**/**4j′** (%)	**5j**+**5j′** (%)	**6j**+**6j′** (%)
30	98/02	00	00	13/13	35	39
40	20/09	33	38			
60	14/13	26	47			
30 (annealed)	98/02	00	00			

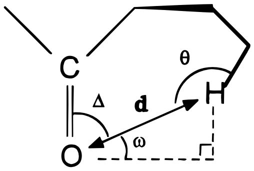

Figure 5. Definition of geometric parameters **d**, *ω*, Δ, and *θ* for intramolecular *γ*-hydrogen atom abstraction.

in the case of diketone **1e**, there is somewhat less cleavage in the solid state above the transition point than in solution. Another interesting observation is that there appears to be considerable "softening" of the crystal lattice just below the transition point of 34 °C in the case of diketone **1d**. At 30 °C, the product distribution has already moved well toward that characteristic of the metastable solid phase. Solid state ^{13}C CPMAS NMR spectra taken of diketone **1d** at 30 °C corroborate this view. Such is not the case for diketone **1e**, however. Here, in spite of the fact that the ^{2}H spectra are strongly temperature dependent below the transition point, the photoproduct distribution does not vary much over the same temperature range.

Discussion

Crystal Structure−Reactivity Relationships in Hydrogen Atom Abstraction. As shown in Figure 5, four parameters serve to define the geometry of hydrogen atom abstraction. The first of these is the distance **d** between the abstracting oxygen atom and the hydrogen atom being abstracted. The second is the angle *ω*, which is the degree to which the *γ*-hydrogen atom lies outside the mean plane of the carbonyl group. The third is the angle Δ, defined as the C═O···H angle, and the fourth is *θ*, the C−H···O angle.

Because it is the half-filled nonbonding orbital on oxygen that is involved in the abstraction process,[27] and because this orbital lies in the plane of the carbonyl group, the ideal value of the angle *ω* is 0°. Similarly, the ideal value of the angle Δ should be between 90° and 120°, depending on whether one views the oxygen n-orbital as being a pure 2p atomic orbital (Kasha model[28]) or sp^2 hybridized ("rabbit ear" model). The abstraction distance **d** should lie close to the sum of the van der Waals radii of the abstracting and abstracted atoms, 1.52 Å + 1.20 Å = 2.72 Å in the case of oxygen and hydrogen.[29] Finally, there seems to be general agreement that the optimum value of the angle *θ* is 180°, i.e., linear.[30]

How do the values of these parameters for diketones **1a**−**j** as determined by X-ray crystallography compare with the ideal values? We begin by discussing the 18-membered-ring diketone **1e**, because in this case the high symmetry of the molecule in the solid state simplifies the analysis. Figure 1e shows the crystallographically-derived conformation of this compound as determined by Allinger et al.[3] Of the eight *γ*-hydrogen atoms in the molecule, only four lie within a reasonable distance for abstraction. These are the four "inner" hydrogen atoms for which the value of the abstraction distance **d** is 2.78 Å, and *ω* = 53°, Δ = 82°, and *θ* = 114°. The four "axial" *γ*-hydrogen atoms, for which **d** = 3.87 Å, are almost certainly too far away to be abstracted. In analyzing the photoreactivity of the remaining diketones, we shall assume that a value of **d** > 3.50 Å eliminates a hydrogen atom from consideration, and only those hydrogen atoms for which **d** ≤ 3.50 Å will be discussed.

Thus for the inner hydrogens of diketone **1e**, three of the four solid state parameters (**d**, Δ, and *θ*) are reasonably close to their ideal values, but the fourth (*ω*) is quite far off. This is, as we shall see, a common feature of the macrocyclic diketones, as indeed it is for other Norrish type II systems that react in the solid state.[4] Wagner and Park[31] have suggested a $\cos^2 \omega$ dependence of the hydrogen abstraction rate constant. In the case of diketone **1e**, this translates into a rate constant that would be diminished to approximately $^1/_3$ of its optimum value, still more than sufficient to afford healthy photoreactivity.

The 10-membered-ring diketone **1a** as well as the 14-membered-ring homologue **1c** also crystallize in conformations with high symmetry such that there is only one abstractable *γ*-hydrogen atom with **d** < 3.50 Å. The values of **d**, *ω*, Δ, and *θ* for these two compounds are compiled in Table 8 along with the data for the remaining diketones. It is interesting to note that the geometric data for the unreactive 10-membered-ring diketone **1a** are virtually indistinguishable from those for the reactive 14- and 18-membered-ring diketones **1c** and **1e**.

The majority of the diketones studied have solid state conformations that contain two or more symmetry-unrelated *γ*-hydrogen atoms with **d** ≤ 3.50 Å, and in these cases we have no *experimental* way of determining which of the nonequivalent hydrogens is actually abstracted in the solid state. This is the reason we went to the trouble of synthesizing the nondiametric diketone **1j**. In this case, the photoproducts resulting from abstraction of a *γ*-hydrogen atom from the shorter methylene chain are structurally different from those that would be formed by abstraction of a *γ*-hydrogen from the longer chain. Provided, therefore, that we can establish the regioisomeric nature of the solid state photoproducts (as we were, in fact, able to do), we have a method for determining which hydrogen atom(s) are preferentially abstracted. This analysis assumes, of course, that the photoproduct ratios are determined by the relative rates of hydrogen atom abstraction and not by the relative rates of reverse hydrogen transfer, a well-known process of 1,4-hydroxy biradical intermediates in the Norrish type II reaction.[18]

Figure 1j shows the conformation of diketone **1j** in the solid state. Owing to the presence of a C_2 axis, the number of independent *γ*-hydrogen atoms in the molecule is reduced from

---

[27] Turro, N. J. *Modern Molecular Photochemistry*; Benjamin-Cummings: Menlo Park, CA, 1978; Chapter 10.

[28] Kasha, M. *Radiat. Res.* **1960**, *Suppl. 2*, 243. See also: Zimmerman, H. E.; Schuster, D. I. *J. Am. Chem. Soc.* **1962**, *84*, 4527.

[29] Bondi, A. *J. Phys. Chem.* **1964**, *68*, 441. See also: Edward, J. T. *J. Chem. Educ.* **1970**, *47*, 261.

[30] Dorigo, A. E.; Houk, K. N. *J. Am. Chem. Soc.* **1987**, *109*, 2195 and references cited therein.

[31] (a) Wagner, P.; Park, B-S. In *Organic Photochemistry*; Padwa, A., Ed.; Marcel Dekker: New York, 1991; Vol. 11, Chapter 4. (b) Wagner, P. J. *Top. Curr. Chem.* **1976**, *66*, 1. (c) Wagner, P. J.; Zhou, B.; Hasegawa, T.; Ward, D. L. *J. Am. Chem. Soc.* **1991**, *113*, 9640.

Table 8. Crystallographically Derived $C{=}O\cdots H_{\gamma}$ Abstraction Geometries[a]

diketone	hydrogen	**d** (Å)	ω (deg)	Δ (deg)	θ (deg)
ideal		2.72	0	90−120	180
1a	H3	2.74	52	91	113
1b	H6 by O1	2.80	66	74	117
	H6 by O2	2.73	64	78	113
1c	H6	2.71	53	83	116
1d	H6	2.74	53	82	115
	H10	2.92	60	66	118
	H20	2.79	53	82	111
	H24	2.92	60	66	116
1e	H5	2.78	53	82	114
1f	H5	2.70	52	83	115
	H13	3.00	59	63	114
	H23	2.70	52	84	115
	H31	2.99	60	64	115
1g	H16	2.82	52	81	111
	H26	3.10	57	59	114
	H35	2.71	44	88	114
1h	H5	3.12	56	59	115
	H17	2.69	50	84	116
	H27	3.17	55	57	116
	H39	2.67	50	83	118
1i needles	H6	2.73	49	85	115
	H20	3.26	57	58	100
1i plates	H5	3.30	52	53	115
	H20	2.76	52	82	113
1j	H6	2.99	59	66	117
	H10	2.72	53	81	116

[a] γ-Hydrogen atoms for which **d** > 3.50 Å are not included in this table. The atom numbering is that used in Figure 1. Data for diketone **1b** are MM2 derived (see text).

Table 9. Average Values for **d**, ω, Δ, and θ for Reactive and Unreactive γ-Hydrogen Atoms

γ-hydrogen	**d** (Å)	ω (deg)	Δ (deg)	θ (deg)
reactive[a]	2.74 ± 0.04	53 ± 5	83 ± 4	115 ± 2
unreactive[b]	3.08 ± 0.14	58 ± 3	61 ± 4	114 ± 5

[a] Average value with standard deviation for all γ-hydrogens with **d** ≤ 2.82 Å (16 total). [b] Average value with standard deviation for all γ-hydrogens with 3.50 Å ≥ **d** > 2.82 Å (10 total).

eight to four, and of these, two have **d** values above 3.50 Å. As a result, we need to consider only H6 on the shorter methylene chain and H10 on the longer. The **d** values for these hydrogens are 2.99 and 2.72 Å, respectively, which predict that H10 should be abstracted in preference to H6. As well, the angular parameters associated with H10 ($\omega = 53°$, $\Delta = 81°$, $\theta = 116°$) are slightly more favorable than those for H6 ($\omega = 59°$, $\Delta = 66°$, $\theta = 117°$). How does the prediction of preferential abstraction of a γ-hydrogen atom from the longer methylene chain in the solid state compare with reality? The agreement is excellent. As indicated in Table 1, cyclobutanol **4** resulting from such an abstraction is the *exclusive* photoproduct obtained when crystals of diketone **1j** are photolyzed. The structural assignment in this case, which rests on an X-ray crystal structure determination, is unassailable. We postpone to a later section of this paper a discussion of the possible reasons for the very high preference for stereoselective cyclobutanol formation in the solid state photoreactions.

Based on the results with diketone **1j**, it appears that we may be able after all to identify which γ-hydrogen atoms are abstracted in the solid state photoreactions. This conclusion is supported by the photochemical results with the needle dimorph of diketone **1i**. The structure−reactivity correlation to be developed later leads to the prediction that, in this case, abstraction of H6 should lead to a *trans*-cyclobutanol photoproduct, whereas abstraction of H20 should afford the *cis* isomer. Since *trans* is by far the major product (Table 1), H6 is identified as the stereoelectronically favored γ-hydrogen atom. In accordance with this conclusion, H6 (**d** = 2.73 Å) has much more favorable distance and angular parameters than H20 (**d** = 3.26 Å, Table 4).

We take the results with diketones **1j** and **1i** (needles) as a strong indication that, at least in the solid state, the photoproduct ratios reflect a kinetic preference for initial abstraction of the stereoelectronically favored γ-hydrogen atom. The alternative argument—that the more distant hydrogen atom is abstracted at a comparable rate and then returned to its carbon atom faster than the 1,4-hydroxy biradical can cleave or cyclize—is counterintuitive and not required by the experimental results.[32a] The one exception to this generalization among the compounds studied in this work is the 10-membered-ring diketone **1a**, whose failure to form products in the solid state we feel is due to rapid reverse hydrogen atom transfer in the 1,4-hydroxy biradical intermediate (*vide infra*).

For the plate dimorph of diketone **1i**, *cis*-cyclobutanol is predicted (and observed) regardless of which of the two possible γ-hydrogen atoms is abstracted (*vide infra*). In this case, therefore, the photochemical results are not helpful in establishing abstraction selectivity, but it seems virtually certain, based on the geometric data for H5 (**d** = 3.30 Å) and H20 (**d** = 2.76 Å), that the latter hydrogen is the one abstracted in the solid state photoreaction. A similar situation applies in the case of diketones **1b**, **1d**, **1f**, **1g**, and **1h**. For each compound, the stereoselectivity of cyclobutanol formation in the solid state provides no information on the selectivity of hydrogen atom abstraction, but based on the geometric data, we may tentatively conclude that the γ-hydrogen atoms with **d** ≤ 2.82 Å are abstracted preferentially, since in every case these are the hydrogen atoms that also have the most favorable values of ω, Δ, and θ. Using all the data in Table 8, if we divide the hydrogen atoms into two categories, those with **d** > 2.82 Å ("unreactive") and those with **d** ≤ 2.82 Å ("reactive"), and then average the geometric data in each category, we arrive at the results shown in Table 9.

These data are, for three reasons, only roughly applicable to the situation in the excited state. First of all, it is likely that diketones **1a**−**1j**, being aliphatic in nature, have carbonyl carbon atoms that are significantly pyramidalized in their n,π^* excited states,[32b] although it is interesting to speculate that the crystalline environment may limit pyramidalization to a considerable extent. Secondly, it is well-known that excitation lengthens carbonyl bonds by about 0.1 Å.[33] A third factor that makes the crystal structure−reactivity correlations less than exact concerns the fact that crystallographically-determined C−H bond lengths are consistently underestimated by approximately 0.1 Å. This is due to the fact that, in the case of hydrogen atoms, the X-rays are diffracted primarily by the electrons in the C−H bonds. This factor also leads to differences between the values of **d** determined crystallographically and those calculated by molecular mechanics methods. We continue to use molecular

---

(32) (a) The results of photolyzing diketone **1j** in solution indicate that the applicability of this conclusion to the *liquid phase*, where photoproduct structure may hide significant variations in the actual excited state reactivity, is less certain. Nevertheless, an interesting analogy is found in the work of Burke et al. (Burke S. D.; Silks, L. A., III; Strickland, S. M. S. *Tetrahedron Lett.* **1988**, *23*, 2761), who showed that relative O···H abstraction distances control regioselectivity in the Barton reaction, a ground state version of the photochemical type II process. (b) This likelihood is based in part on the experimentally well-established fact that formaldehyde adopts a pyramidal geometry in its n,π^* singlet and triplet excited states (Moule, D. C.; Walsh, A. D. *Chem. Rev.* **1975**, *75*, 67 and references therein). *Ab initio* calculations by Sauers and Edberg[40] on the triplet state geometries of aliphatic aldehydes and ketones support the picture of a partially (22−45°) pyramidalized carbonyl group.

(33) Chandler, W.; Goodman, L. *J. Mol. Spectrosc.* **1970**, *35*, 232.

parameters based on X-ray H sites for the following reasons: (i) all our previous structure−reactivity correlations have been based on X-ray H sites, so that a change now would make comparisons with previous discussions confusing; (ii) since C−H···O angles are all near 115°, a correction of +0.1 Å to the C−H distances would simply decrease all O···H distances by about 0.05 Å; (iii) the O···H (X-ray) distances, i.e., from oxygen to the centers of the hydrogen electron clouds, may in fact be more relevant than distances to the hydrogen nucleus.

Despite these uncertainties it is remarkable that the values of **d** for the "reactive" hydrogen atoms in diketones **1a**−**1j** (average **d** = 2.74 ± 0.04 Å) are so internally consistent and lie so close to the sum of the van der Waals radii for oxygen and hydrogen (2.72 Å). This plus the fact that very similar structure−reactivity correlations have been found for other completely unrelated crystalline type II systems[4] lends credence to the idea that such data can be used in a *predictive* way to gauge the success of potential hydrogen atom abstraction photoreactions, since values of **d**, ω, Δ, and θ can now be estimated readily with the help of molecular force field calculations. A final point is that while the present results indicate that abstraction will be favored in competitive systems for hydrogen atoms located near the sum of the van der Waals radii, this does not mean that hydrogen abstraction is limited to such distances. We have shown that values of **d** as great as 3.1 Å (albeit with relatively favorable ω and Δ values) can be tolerated in the solid state,[4] and this remains our best current estimate of the approximate upper limit to intramolecular hydrogen atom abstraction by ketonic oxygen.

Another structure−reactivity correlation that can be developed from the present results concerns the overall geometry of the six-membered transition state for γ-hydrogen atom abstraction. The well-known prevalence of γ-hydrogen abstraction over the corresponding β and δ processes was originally attributed by Wagner *et al.* to enthalpic factors associated with a strain-free, chairlike, cyclic six-atom transition state.[34] Later theoretical studies by Dorigo and Houk clarified the important role that entropic factors play in determining regioselectivity as well.[30] Non-chair geometries can be tolerated in conformationally rigid systems, however, and we have shown that even in relatively flexible α-cycloalkylacetophenone derivatives, γ-hydrogen atom abstraction frequently occurs through boatlike or twist-boatlike rather than chairlike six-atom geometries.[35] Inspection of the conformational drawings shown in Figure 1 reveals that a similar situation obtains in the case of macrocyclic diketones **1a**−**1j**. In every case but one, the stereoelectronically favored γ-hydrogen atoms (**d** ≤ 2.82 Å) are associated with boatlike abstraction geometries. The lone exception is H6 in diketone **1b**, which, at **d** = 2.80 Å, is in a chairlike position.

The boatlike abstraction geometry is the result of the conformations adopted by the macrocyclic diketones in the crystalline state. Unlike acyclic ketones, which are known to prefer extended *anti* conformations in the solid state[36] (conformations that render γ-hydrogen atom abstraction sterically impossible), the macrocyclic diketones generally crystallize in rectangular conformations that require gauche arrangements at the corner positions. The carbonyl groups prefer to be located next to the corner positions[37a] such that the nearest γ-hydrogen atom is arranged as shown in Figure 6, which is based on the crystal structures of the 16- and 18-membered-ring diketones **1d** and **1e**. The β-carbon represents a corner position,[37b] and the boatlike six-atom geometry is clearly evident when the dotted lines indicating abstraction are included. Pyramidalization of the carbonyl carbon in the excited state can either increase or decrease **d** depending on the direction in which the oxygen moves, but we have no way of monitoring the extent or direction of this motion. As noted earlier, geometries similar to the ones shown in Figure 6 can be accommodated for aryl ketones that do not pyramidalize upon excitation.[35]

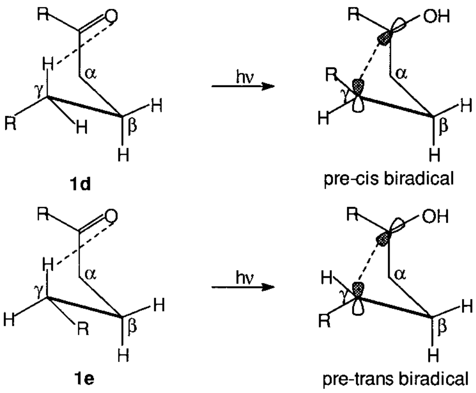

Figure 6. Partial conformations of diketones **1d** and **1e** leading to pre-*cis* and pre-*trans* 1,4-biradicals.

Crystal Structure−Reactivity Relationships in Biradical Reactivity. In this section we discuss possible reasons for the findings (Table 1) that (a) type II cyclization is much more prevalent in the crystalline state than in solution and (b) the cyclization reactions in the solid state are much more stereoselective than those in solution. As in the case of the structure−reactivity correlations derived for hydrogen atom abstraction, we shall make extensive use of geometric data derived from the X-ray crystal structures.

A key assumption in the arguments that follow is that hydrogen abstraction occurs in the crystalline state with minimal conformational changes, so that the 1,4-hydroxy biradical intermediates that are formed closely resemble the starting diketones in shape and structure. Let us take the 16-membered-ring diketone **1d** as a representative example. As shown in Figure 6, abstraction of the stereoelectronically favored γ-hydrogen atom (H6, **d** = 2.74 Å, dotted line) would lead to the corresponding biradical, which is assumed to differ from the starting diketone only in the conversion of the carbonyl group to a protonated ketyl radical and in the change of hybridization of the γ-carbon atom from sp^3 to sp^2; the p-orbital at this center is assumed to lie perpendicular to the $C\beta-C\gamma-C\delta$ plane. From this biradical, least motion closure involving overlap of the orbital lobes that are directed toward one another (dotted line) would lead to a cyclobutanol in which the unabstracted γ-hydrogen atom and the hydroxyl group end up on the same side of the 4-membered ring, i.e., *cis*-cyclobutanol **4d**, which is the major photoproduct (89%) in the crystalline state. Formation of a *trans*-cyclobutanol in this case would necessitate inversion of configuration at either the carbonyl carbon or the γ-carbon—motions requiring substantial distortions of the molecular framework that are resisted by the solid state environment.

The lack of 1,4-biradical cleavage in the crystalline state can be related to the poor overlap of the p-orbital at the hydroxyl-bearing carbon atom with the central $C\alpha-C\beta$ bond. It is

---

(34) Wagner, P. J.; Kelso, P. A.; Kemppainen, A. E.; Zepp, R. G. *J. Am. Chem. Soc.* **1972**, *94*, 7500.

(35) Scheffer, J. R.; Trotter, J.; Omkaram, N.; Evans, S. V.; Ariel, S. *Mol. Cryst. Liq. Cryst.* **1986**, *134*, 169.

(36) Slivinskas, J. A.; Guillet, J. E. *J. Polym. Sci., Polym. Chem. Ed.* **1973**, *11*, 3043.

(37) (a) Anet, F. A. L.; Cheng, A. K.; Krane, J. *J. Am. Chem. Soc.* **1973**, *95*, 7877. (b) Since the 18-membered-ring diketone **1e** does not have a rectangular conformation in the solid state, the β-carbon in this case is not strictly speaking a corner position. Nevertheless, Figure 6 depicts the situation accurately.

Table 10. Crystallographically Derived Biradical Geometries and Predicted Behavior[a]

		cyclobutanol				
diketone	hydrogen	predicted	observed	φ_1 (deg)	φ_4 (deg)	**D** (Å)
1a	H3	*cis*	no rxn	68	30	3.27
1b	H6 by O1	*cis*	*cis*	12	85	3.12
	H6 by O2	*cis*		56	21	3.13
1c	H6	*cis*	*cis*	66	25	3.16
1d	H6	*cis*	*cis*	67	24	3.16
	H20	*cis*		68	25	3.16
1e	H5	*trans*	*trans*	69	90	3.17
1f	H5	*cis*	*cis*	71	24	3.16
	H23	*cis*		69	25	3.16
1g	H16	*trans*	*trans*	69	86	3.14
	H35	*trans*		81	87	3.19
1h	H17	*cis*	*cis*	74	25	3.18
	H39	*cis*		72	26	3.15
1i needles	H6	*trans*	*trans*	73	86	3.18
1i plates	H20	*cis*	*cis*	71	24	3.17
1j	H10	*cis*	*cis*	66	26	3.13

[a] γ-Hydrogen atoms for which $\mathbf{d} > 2.82$ Å are not included in this table. The atom numbering is that used in Figure 1. Data for diketone **1b** are MM2 derived.

generally agreed that cleavage of 1,4-biradicals requires a near-coplanar alignment of the central carbon−carbon bond with the participating p-orbitals,[18] and in the case of the biradical formed from diketone **1d** (Figure 6), the p-orbital on the hydroxyl-bearing carbon is 67° out of alignment with this bond. We designate this angle as φ_1. The p-orbital on the γ-carbon, on the other hand, is better situated for cleavage, but is still 24° misaligned (φ_4). These angles are derived from the crystal structure of diketone **1d** assuming that the orbitals involved are orthogonal to an unaltered carbon framework. Thus, since the orbitals are well oriented for ring closure, and the two carbon atoms involved in bond formation are separated by only $\mathbf{D} = 3.16$ Å (significantly less than 3.40 Å, the sum of the van der Waals radii for two carbon atoms), it is not surprising that cyclization predominates in the crystalline state.

Exactly the same conclusion is reached if we analyze the biradical formed by abstraction of the other stereoelectronically accessible hydrogen atom (H20, $\mathbf{d} = 2.79$ Å) in diketone **1d**. Once again, *cis*-cyclobutanol is predicted, and the values of φ_1, φ_4, and **D** are 68°, 25°, and 3.16 Å, respectively, almost identical to the values associated with the abstraction of H6.

Let us now consider the case of a diketone whose photolysis in the solid state leads predominantly to a *trans*-cyclobutanol. The 18-membered-ring homologue **1e** is such a compound. Here it is readily apparent (Figure 6) that the non-abstracted γ-hydrogen atom and the carbonyl oxygen atom are *anti* to one another in the crystalline state, so that a least motion hydrogen abstraction/cyclization process involving retention at both centers (bonding as shown by the dotted line, Figure 6) should lead to a *trans*-cyclobutanol, as observed. In this case, the values of φ_1, φ_4, and **D** are 69°, 90°, and 3.17 Å, all consistent with a species that should prefer to cyclize rather than cleave.

Similar analyses successfully account for the solid state photochemistry of all of the diketones studied in this work with the exception of the photochemically inert 10-membered-ring diketone **1a**. At this point, rather than going through each case separately in detail, the predicted and observed cyclobutanol stereochemistries as well as the values of φ_1, φ_4, and **D** for each diketone are compiled in Table 10. Data for biradicals that would be formed by abstraction of remote ($\mathbf{d} > 2.82$ Å) hydrogen atoms are not included.

There is a remarkable degree of internal consistency in the values of φ_1, φ_4, and **D**. For diketones that afford primarily *cis*-cyclobutanols upon irradiation in the crystalline state, one angle is large, typically around 70°, and the other is smaller, characteristically around 25°; for diketones that lead to *trans*-cyclobutanols, both angles are large (*ca*. 70° and 90°). Drawings of these so-called "pre-*cis*" and "pre-*trans*" biradicals are shown in Figure 6. The consistency in the structural data and its ability to account correctly for the type and stereochemistry of the photoproducts argue against the intervention of supramolecular crystal lattice forces in governing the solid state photochemistry, forces that typically vary considerably from crystal to crystal. Rather, the role of the solid state in these reactions appears to be that of a passive, highly viscous, but essentially isotropic medium.

Solid State Versus Solution Phase Results: 1,6-Cyclodecanedione (1a). In the sections that follow we compare the photochemical behavior of the 10- to 16-membered-ring diketones in solution and the solid state with the help of MM2 calculations that reveal the conformational preferences of these molecules in solution. We begin with 1,6-cyclodecanedione (**1a**). The geometric data for this compound listed in Tables 8 and 10 differ very little from the corresponding data for the reactive diketones and predict formation of a *cis*-cyclobutanol, yet this compound is completely unreactive in the solid state. Our initial idea was that, despite an apparently favorable abstraction geometry, there might be some unexpectedly large increase in steric energy associated with γ-hydrogen abstraction in this the smallest of the diketones investigated. Sauers *et al.* have recently developed an MM2-based program for calculating the steric energies of intramolecular hydrogen abstraction reactions of alkanone triplet states using *ab initio*-derived transition state structures,[38] and Professor Sauers kindly agreed to subject diketone **1a** in its solid state conformation to such an analysis. The results of this analysis indicated that diketone **1a** should experience little difficulty in abstracting a γ-hydrogen atom−indeed that it should react as well as, if not better than, cyclodecanone itself, which Sauers and Huang had shown undergoes γ-hydrogen abstraction in *tert*-butyl alcohol to afford *cis*-1-hydroxybicyclo[6.2.0]octane as the major product.[15,39] More recently, Sauers and Edberg have analyzed intramolecular hydrogen atom abstraction reactions through the use of *ab initio* calculations,[40] and application of this methodology to diketone **1a** likewise predicts that it should be photochemically reactive.[41]

The failure of diketone **1a** to react in the solid state is, therefore, almost certainly associated with the second step, biradical closure. Since the cyclization geometry is normal for the macrocyclic diketones (Table 10), there must be some additional factor at play in this case. We would like to suggest that this factor is steric strain associated with closure to an 8-membered ring. Enthalpies of activation for the formation of 8-membered rings are known to be particularly high owing to transannular interactions between hydrogen atoms,[42] and with reference to the biradical formed by photolysis of diketone **1a**, closure with overall retention of conformation as enforced by the solid state medium would involve the development of a very severe transannular repulsive interaction between H2 and H8 on the 8-membered ring. In addition, H15 on the newly formed 4-membered ring would be brought into very close proximity to H3 on the 8-membered ring. Structural drawings depicting

---

(38) Sauers, R. R.; Krogh-Jespersen, K. *Tetrahedron Lett.* **1989**, *30*, 527.

(39) The stereochemistry of this cyclobutanol was not assigned by Sauers and Huang,[15] but they reported that it gave rise to a signal at 48.22 ppm in the ^{13}C NMR spectrum, and based on our work (see section on characterization of photoproducts), this can be taken as indicating a *cis* ring junction.

(40) Sauers, R. R.; Edberg, L. A. *J. Org. Chem.* **1994**, *59*, 7061.

(41) Lewis, T. J.; Rettig, S. J.; Sauers, R. R.; Scheffer, J. R.; Trotter J.; Wu, C.-H. *Mol. Cryst. Liq. Cryst.* **1996**, *277*, 289.

(42) Illuminate, G.; Mandolini, L. *Acc. Chem. Res.* **1981**, *14*, 95.

Scheme 3

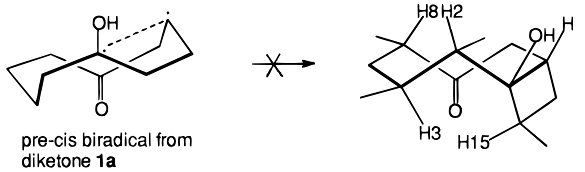

these interactions are shown in Scheme 3. With closure thus retarded and cleavage made difficult due to poor orbital alignment, the biradical reverts to starting material and the diketone appears to be photochemically inert.

But what about the situation in solution? Is diketone **1a** truly unreactive in this medium or does it (as in the solid state) just give the appearance of being photoinert? To help answer these questions, we turned to a molecular mechanics analysis of the preferred conformations of diketone **1a**.[43] These calculations revealed that diketone **1a** has three conformations within a 20 kJ/mol energy window above the global minimum: conformer **A** (the global minimum), conformer **B** (relative energy 9.9 kJ/mol), and conformer **C** (relative energy 11.9 kJ/mol). Drawings of these conformations are given in Figure 7. As can be seen by comparison with Figure 1a, it is conformer **C** that closely resembles the conformation adopted by diketone **1a** in the crystalline state.[44] The other two conformations are very different, and in particular it can be seen that, for the minimum energy conformation **A**, γ-hydrogen atom abstraction is sterically impossible: the γ-hydrogens are either on the wrong side of the ring or are pointing directly away from the oxygen atoms ($\mathbf{d} \gg 3.50$ Å). Conformer **B** has one potentially abstractable hydrogen atom (H13, $\mathbf{d} = 2.52$ Å), and like conformer **C**, should be photoreactive in *tert*-butyl alcohol.

Interestingly, conformer **A** is well arranged for δ-hydrogen abstraction, with calculated values of $\mathbf{d} = 2.67$ Å, $\omega = 63°$, $\Delta = 92°$, and $\theta = 102°$. Application of the Sauers' transition state analysis program to this process, however, indicates that δ-abstraction is not favorable,[45] and another factor that disfavors such a reaction in the case of diketone **1a** is that the δ-hydrogen atoms are deactivated inductively by being next to the second carbonyl group.[18] δ-Hydrogen abstraction is also possible for the solid state conformer of diketone **1a** (crystallographic $\mathbf{d} = 2.81$ Å, $\omega = 99°$, $\Delta = 76°$, and $\theta = 134°$) but is disfavored not only inductively but by an unfavorable value of the angle ω. A plausible reason for the lack of reactivity of diketone **1a** in solution thus stands revealed: in this medium, the great majority of the reactant molecules (approximately 97% if one uses the calculated energies) adopt a conformation (**A**) for which both γ- and δ-hydrogen atom abstraction are most unlikely.

Raising the temperature should increase the concentrations of the potentially reactive conformers **B** and **C**, albeit only slightly. Nevertheless, we thought it worthwhile to try a photolysis in *tert*-butyl alcohol at 80 °C. At this temperature, the conformer population is predicted to be approximately 95% **A**, 3% **B**, and 2% **C**. By carrying out the photolysis under these conditions in the presence of a photochemically unreactive internal standard (heptadecane), it was possible to detect a very slow loss of parent diketone. GC analysis of the reaction mixture showed the development of a number of very small peaks, none of which integrated to more than a few tenths of a percent of the total. Control experiments demonstrated that 1,6-cyclodecanedione is stable in hot *tert*-butyl alcohol in the dark.

Our molecular mechanics calculations on diketone **1a** confirm the hypothesis advanced by Alvik, Borgen, and Dale[6] that the C_{2h} symmetric "crown" or twist chair−chair−chair conformer **A** is the major conformer present in solution. This hypothesis was based on dipole moment measurements and on the finding that the infrared spectrum of diketone **1a** in solution was very different from that in the solid state. Later work by Anet *et al.* on the variable-temperature ^{1}H and ^{13}C NMR spectra of **1a** was also consistent with the Dale hypothesis.[46] However, two questions remain: (1) Why is the higher energy conformer **C** preferred in the crystalline state, and (2) why does conformer **A** have a lower overall energy than the boat−chair−boat conformer **C**? This last question is particularly intriguing in view of the fact that both cyclodecane and cyclodecanone have solid state conformations very similar to that of **C**, i.e., of the diamond lattice boat−chair−boat type.[47]

Alvik, Borgen, and Dale suggested that the crown conformation **A** is favored by attractive C−H···O interactions between the carbonyl oxygen atoms and the δ-hydrogen atoms on the opposite side of the 10-membered ring.[6] This was a prescient suggestion since, at the time, the very existence of C−H···O interactions was the subject of considerable debate, and although today their presence is well accepted,[48] they are almost always invoked to explain crystal packing phenomena, not fluid phase conformational equilibria. They have, however, been suggested to be important in determining rotamer populations in some instances,[49] and on the basis of MP2/6-31G* calculations on the interaction between methane and formaldehyde, Wiberg *et al.* concluded that there is an energy minimum at a C−H···O distance of 2.58 Å.[50a] It is also well established that C−H···O interactions become stronger as the C−H bonds become more acidic,[50b] and this factor increases the likelihood of C−H···O interactions in the case of conformer **A**, where the hydrogens in question are α to the carbonyl groups.

We would like to propose that there is a second interaction that is important in stabilizing crown conformer **A** in solution: the dipole−dipole attraction between the two carbonyl groups. As can be seen from inspection of Figure 7, the ketone groups of conformer **A** have a coplanar, head-to-tail orientation with a nonbonded C···O distance (MM2) of 3.08 Å, somewhat less

---

(43) Monte Carlo multiple minimum conformational searches were carried out on a Silicon Graphics Personal Iris 4D computer for the 10-, 12-, 14-, and 16-membered-ring diametric diketones by using the MM2 force field in MACROMODEL, a molecular modeling program developed by the following: (a) Chang, G.; Guida, W. C.; Still, W. C. *J. Am. Chem. Soc.* **1989**, *111*, 4379. (b) Mohamadi, F.; Richards, N. G. J.; Guida, W. C.; Liskamp, R.; Lipton, M.; Caufield, C.; Chang, G.; Hendrickson, T.; Still, W. C. *J. Comput. Chem.* **1990**, *11*, 440.

(44) In the MM2-derived conformation **C**, the angular parameters of the γ-hydrogen ($\omega = 52°$, $\Delta = 93°$, $\theta = 113°$) are very close to those found by X-ray ($\omega = 52°$, $\Delta = 91°$, $\theta = 113°$), but the O···H contact distance (2.54 Å) is quite short compared to that of the solid state conformer (2.74 Å).

(45) Sauers, R. Personal communication.

(46) Anet, F. A. L.; St. Jacques, M.; Henrichs, P. M.; Cheng, A. K.; Krane, J.; Wong, L. *Tetrahedron* **1974**, *30*, 1629.

(47) (a) Dunitz, J. D. In *Perspectives in Structural Chemistry*; Dunitz, J. D., Ibers, J. A., Eds.; Wiley: New York, 1968; Vol. 2, pp 1−70. (b) Groth, P. *Acta Chem. Scand.* **1976**, *A30*, 294. The latter paper is concerned with the crystal structure of cyclodecanone at −160 °C (cyclodecanone melts at 24 °C) and shows that this compound crystallizes in a boat−chair−boat conformation closely resembling that of **C**. Not surprisingly, therefore, the crystallographically-derived γ-hydrogen atom abstraction parameters for cyclodecanone are similar to those of diketone **1a** ($\mathbf{d} = 2.70$ Å, $\omega = 33°$, $\Delta = 83°$, $\theta = 116°$, $\varphi_1 = 57°$, $\varphi_4 = 25°$, $\mathbf{D} = 3.14$ Å). Molecular mechanics calculations indicate that this conformer lies 0.9 kJ/mol above the global minimum twist boat−chair−chair conformer. Both conformers possess abstractable γ-hydrogen atoms, thus accounting for the type II reactivity of cyclodecanone in *tert*-butyl alcohol.[15]

(48) (a) Desiraju, G. R. *Acc. Chem. Res.* **1991**, *24*, 290. (b) Taylor, R.; Kennard, O. *J. Am. Chem. Soc.* **1982**, *104*, 5063.

(49) (a) Zushi, S.; Kodama, Y.; Nishihata, K.; Umemura, K.; Nishio, M.; Uzawa, J.; Hirota, M. *Bull Chem. Soc. Jpn.* **1980**, *53*, 3631. (b) Gough, K. M.; Millington, J. *Can. J. Chem.* **1995**, *73*, 1287.

(50) (a)Wiberg, K. B.; Waldron, R. F.; Schulte, G.; Saunders, M. *J. Am. Chem. Soc.* **1991**, *113*, 971. (b) Pedireddi, V. R.; Desiraju, G. R. *J. Chem. Soc., Chem Commun.* **1992**, 988.

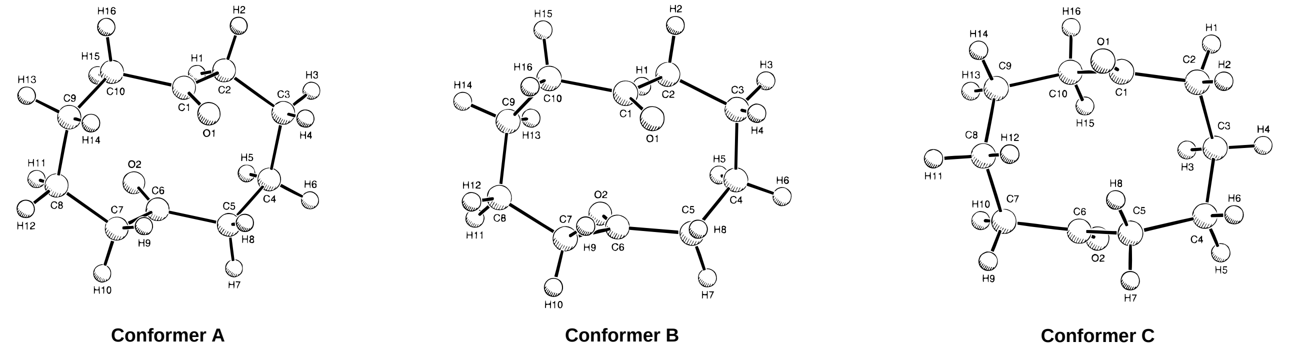

Conformer A **Conformer B** **Conformer C**

Figure 7. MM2-derived conformations **A**, **B**, and **C** of diketone **1a**.

than the sum of the van der Waals radii for carbon and oxygen (3.22 Å). The corresponding distance in conformer **C** is 4.19 Å (X-ray value) and those for conformer **B** (which lacks symmetry) are 3.41 and 3.66 Å (MM2). As a result, the electrostatic component of the total strain energy from the MM2 calculations is relatively large and negative for conformer **A** (−6.13 kJ/mol) compared to the values for conformers **B** (−1.98 kJ/mol) and **C** (0.22 kJ/mol). This explanation nicely rationalizes the fact that cyclodecane and cyclodecanone, for which attractive intramolecular carbonyl interactions are obviously impossible, have lower energy boat−chair−boat conformations, which are favored on purely steric grounds. The C═O···C═O interaction does not show up in the infrared spectrum of diketone **1a**, however. In carbon tetrachloride, this material has the same carbonyl stretching frequency (1713 cm^{-1}) as diones **1c** and **1d**. Similarly, the fluorescence spectra of diketones **1a**, **1c**, and **1d** are virtually identical.

As mentioned above, conformationally flexible molecules generally crystallize in or near their lowest energy conformations, yet 1,6-cyclodecanedione prefers the significantly higher energy boat−chair−boat conformer **C** in the solid state. One possible explanation is that conformer **C** might be favored in the crystal by attractive *inter*molecular C═O···C═O interactions. The carbonyl groups of conformer **C** (unlike those of conformer **A**) are free of intramolecular electrostatic contacts, and might therefore be more available to attract other carbonyl groups intermolecularly. The crystal structure of 1,6-cyclodecanedione does not support this picture, however. The packing diagram shows that the carbonyl groups on adjacent molecules are non-interacting.

In their 1972 paper, Dale *et al*. noted that, compared to other diametric diketones, 1,6-cyclodecanedione had unusually large values of the enthalpy and entropy of melting, thus indicating the presence of particularly strong packing forces.[6] Our X-ray crystallographic results support this conclusion. The calculated crystal density of 1,6-cyclodecanedione (**1a**) is 1.240 g/cm^3, approximately 15−20% higher than the other diametric diketones whose crystal structures we determined (see Table 3). The packing forces that favor the crystallization of 1,6-cyclodecanedione in the higher energy boat−chair−boat form **C** are probably related to the fact that this conformer is more spherical and fills space better than the more extended conformers **A** and **B**. In addition, and perhaps more importantly, the crystal structure indicates that there is an extensive network of close *inter*molecular C═O···H contacts in this case. Each oxygen atom of conformer **C** has no less than five C═O···H contacts under 3 Å with a neighboring molecule. The three closest of these, at 2.65, 2.77, and 2.86 Å, involve interactions with the relatively acidic α-hydrogens. These contacts probably account for the unusually low carbonyl stretching frequency exhibited by 1,6-cyclodecanedione in the solid state (1688 cm^{-1}) compared to those of other diametric diketones (1700−1705 cm^{-1}).

Solid State Versus Solution Phase Results: 1,7-Cyclododecanedione (1b). Turning now to the 12-membered-ring diketone **1b**, we recall that the crystal structure of this material could not be determined, and that it was assumed that the square or [3333] minimum energy conformation identified by MM2 (Figure 1b) is the conformation present in the crystalline state. This assumption is based on the work of Dale *et al*.,[6] who concluded from dipole moment measurements and conformational arguments that the [3333] structure with the carbonyl groups in non-corner positions should be the preferred conformer in solution, and since the solid state and solution phase infrared spectra were identical, that this was the conformer present in the crystal as well. Further support for this conclusion comes from X-ray,[51] NMR,[52] and molecular modeling[53] studies on the corresponding monoketone, cyclododecanone, which show that this compound has the same [3333]-2-one conformation in solution and the solid state.

Our MM2 calculations on diketone **1b** found five additional conformations (not shown) within a 10-kJ/mol window above the global minimum at relative energies of 5.7, 7.9, 9.2, 9.7, and 9.7 kJ/mol. In every case, including the minimum energy conformation, the calculated structure was such that *cis*-cyclobutanol was predicted. The only exception was one of the 9.7-kJ/mol conformers, where one of the γ-hydrogens was oriented so as to lead to a *trans*-cyclobutanol. In view of these findings, it is not suprising that irradiation of diketone **1b** gives a very high proportion of *cis*-cyclobutanol in solution, as it does in the solid state. Interestingly, solution phase photolysis of the corresponding monoketone, cyclododecanone, also leads mainly to a *cis*-cyclobutanol derivative.[7−9]

Solid State Versus Solution Phase Results: 1,8-Cyclotetradecanedione (1c). The solid state photochemistry of the 14-membered-ring diketone **1c** is unique among the compounds studied in that cyclobutanol formation is relatively non-stereoselective (*cis*:*trans* = 2:1) and a significant amount of cleavage (13%) is observed. As in the case of the 12-membered-ring diketone, the solution photoproduct ratios are very similar to those observed in the solid state. Molecular mechanics calculations in the case of the 14-membered-ring diketone **1c** reveal an unusual situation in which there are two minima that differ in energy by only 0.3 kJ/mol, but which have very different conformations. The lower of the two is virtually identical to the solid state conformer, and the other (conformer **D**) has the unsymmetrical conformation shown in Figure 8. We note that the solid state conformer is of the [3434] type predicted by Dale *et al*., with the carbonyl groups situated in the middle of the longer segment.[6] Three other conformers (not shown) were also located at relative energies of 2.0, 2.8, and 4.5 kJ/mol.

---

(51) Groth, P. *Acta Chem. Scand. A* **1979**, *33*, 203.
(52) Rawdah, T. N. *Tetrahedron* **1991**, *47*, 8579.
(53) Rawdah, T. N.; El-Faer, M. Z. *Tetrahedron* **1990**, *46*, 4101.

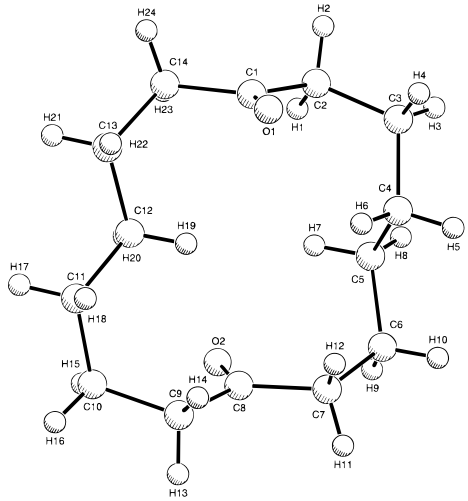

Figure 8. MM2-derived conformation **D** of diketone **1c**.

Conformer **D** can be generated from the solid state conformer by 120° rotations about the C10−C11 and C12−C13 bonds in what should be a relatively low energy process. As can be seen, this conformer has one γ-hydrogen atom (H19), abstraction of which will lead to a *trans*-cyclobutanol. It is tempting, therefore, to attribute the unusual decreased stereoselectivity of the photoreaction of diketone **1c** in the crystalline state to the presence of conformer **D** in the crystals prior to the photoreaction or to the formation of conformer **D** in the vicinity of reaction sites in the partially photolyzed crystal. The first possibility seems unlikely, as there is no indication from the crystal structure of the presence of a second conformational isomer, nor does diketone **1c** undergo a detectable low-temperature solid−solid phase transition. It is, however, conceivable that such a phase transition could be induced by the presence of low levels of foreign molecules (the photoproducts) that do not fit well in the parent lattice. Literature precedent for a photoproduct-induced phase transition (from liquid crystalline to solid) comes from the work of Weiss *et al.*,[54] and this scenario represents our best rationalization at present for the atypical photobehavior of diketone **1c** in the crystalline state.[55] In the five conformers identified by MM2 within a 5 kJ/mol energy window, there are only three γ-hydrogen atoms in pre-*trans* orientations, one in conformer **D** (Figure 8) and two in the 2.8-kJ/mol conformer (not shown). It is not surprising, therefore, that *cis*-cyclobutanol predominates in solution as well as in the solid state.

Solid State Versus Solution Phase Results: 1,9-Cyclohexadecanedione (1d). The 14-membered-ring diketone **1c** was the largest molecule that we could analyze thoroughly by MM2 in a reasonable length of time on the Silicon Graphics work station available to us; similar calculations on the 16-membered-ring homologue **1d** took an inordinately long time, and we could not be sure that a complete conformational search was achieved. Nevertheless, our preliminary results with the latter diketone showed that the rectangular [3535] solid state conformation is also the MM2 global minimum by 2.0 kJ/mol. This result is in agreement with the prediction of Allinger *et al.*,[56] but not that of Alvik, Borgen, and Dale who, on the basis of qualitative arguments involving $C{=}O\cdots H$ interactions, favored a square [4444] lowest energy conformation for 1,9-cyclohexadecanedione.[6] Our molecular mechanics results further showed that there are no less than 19 additional conformational isomers within a 10 kJ/mol energy window above the minimum, a clear indication that this compound has high conformational mobility relative to the smaller members of the series. The first eight of these conformers have relative energies of 3.6, 4.9, 5.3, 6.3, 6.5, 6.7, 6.8, and 7.6 kJ/mol. Of the ten lowest energy conformers, eight have γ-hydrogen abstraction geometries that predict the exclusive formation of *cis*-cyclobutanol; only the 6.3- and 7.6-kJ/mol conformers have $C{=}O\cdots H$ arrangements for which *trans*-cyclobutanol formation would be expected. Why, then, does the solution phase photolysis of the 16-membered-ring diketone **1d** lead mainly to cleavage (43%) and *trans*-cyclobutanol formation (35%), with only 22% of the product being formed that is predicted from the conformer population (*cis*-cyclobutanol)? The likely answer is that, owing to the greater flexibility of the 16-membered ring, there is at least partial if not full conformational equilibration of the triplet 1,4-hydroxy biradical intermediate during its lifetime, and product formation in this case reflects the relative activation energies of the various processes available to this species (Curtin−Hammett principle). Furthermore, it would appear that the 1,4-hydroxy biradical reacts through non-minimum energy conformations that are particularly favorable for cleavage and *trans*-cyclobutanol formation. If this were not the case, and reactivity was limited to biradical conformations similar to those identified by MM2, *cis*-cyclobutanol formation should still be preferred.[57]

Information on the barriers to conformational isomerization of the homologous cyclic diketones **1a**−**1e** is lacking except for an estimate of $\approx$10 kcal/mol for the 10-membered-ring dione **1a**.[46] For the corresponding 8- to 16-membered-ring *mono*ketones, however, the conformational energy barriers ($\Delta G^{\ddagger}$) have been measured by ^{13}C and ^{1}H NMR and found to be more or less constant between approximately 5.0 and 7.5 kcal/mol.[58] As pointed out by Allinger and co-workers[56] as well as by Anet *et al.*,[59] the major difference in terms of conformational flexibility between medium-sized ring compounds on the one hand and macrocyclic systems on the other lies in what Allinger refers to as their "floppiness" and what Anet terms "libration". To quote Anet, "It seems likely that the conformations of large-ring hydrocarbons are relatively nonrigid, and that librations can occur whereby some torsional angles change by an appreciable amount (say 10°) with only a small increase in strain energy."[59] By floppiness, Allinger means "...that substantial deformations on one side of the molecule can be carried out with essentially no effect on what occurs on the other side,"[3] and that the molecule "...has broad torsional wells, similar to those found in an open chain."[56] We suggest that it is similar floppiness in the 1,4-hydroxy biradicals derived from the

---

(54) Furman, I.; Butcher, R. J.; Catchings, R. M.; Weiss, R. G. *J. Am. Chem. Soc.* **1992**, *114*, 6023.

(55) Specific intermolecular steric interactions resulting from close contacts between molecules in the crystalline state have been shown to be capable of altering solid state photobehavior (see: Ariel, S.; Askari, S.; Evans, S.; Hwang, C.; Jay, J.; Scheffer, J. R.; Trotter, J.; Walsh, L.; Wong, Y.-F. *Tetrahedron*, **1987**, *43*, 1253), and a third possible reason for the lack of solid state photoproduct selectivity in the case of diketone **1c** is that the crystal packing somehow disfavors the formation of the stereoelectronically favored *cis*-cyclobutanol. Inspection of the packing diagrams for this compound, however, revealed no obvious intermolecular contacts that would produce this effect.

(56) Allinger, N. L.; Gorden, B.; Profeta, S., Jr. *Tetrahedron* **1980**, *36*, 859.

(57) In such conformationally complex situations, the role played by conformational memory effects of the type suggested by Scaiano to be important in determining product distributions from triplet 1,4-biradicals is difficult to sort out. The situation is further complicated in the case of the macrocyclic diketones by the fact that the reactions are of mixed singlet/triplet character. Nevertheless, it is entirely possible that the solution phase photoproduct ratios for these compounds are strongly influenced by triplet biradical intersystem crossing rates, and the interested reader is referred to the following: Scaiano, J. C. *Tetrahedron* **1982**, *38*, 819.

(58) Anet, F. A. L.; Cheng, A. K.; Krane, J. *J. Am. Chem. Soc.* **1973**, *95*, 7877.

(59) Anet, F. A. L.; Cheng, A. K. *J. Am. Chem. Soc.* **1975**, *97*, 2420.

Table 11. Final Atomic Coordinates (fractional) and B_{eq} (Å^2)[a]

atom	*x*	*y*	*z*	B_{eq}	atom	*x*	*y*	*z*	B_{eq}	atom	*x*	*y*	*z*	B_{eq}
1a														
O(1)	0.2171(1)	0.1432(2)	0.36461(7)	3.85(4)	C(2)	0.5213(2)	0.0825(2)	0.3055(1)	3.10(4)	C(4)	0.7655(2)	0.2408(2)	0.4679(1)	3.00(4)
C(1)	0.3561(1)	0.0137(2)	0.37001(8)	2.59(4)	C(3)	0.7187(2)	0.0593(2)	0.3692(1)	2.97(4)	C(5)	0.6382(1)	0.2273(2)	0.5653(1)	2.62(4)
1c														
O(1)	1/2	0.3554(5)	0.2560(4)	7.1(2)	C(2)	0.4221(4)	0.2165(6)	0.0968(4)	7.9(3)	C(4)	0.3539(3)	0.4912(8)	0.0713(6)	11.7(4)
C(1)	1/2	0.2719(6)	0.1580(6)	6.0(3)	C(3)	0.3519(3)	0.3199(8)	0.1257(5)	9.4(3)					
1d														
O(1)	0.4556(2)	0.3641(1)	0.3243(2)	5.6(1)	C(5)	0.1641(2)	0.3903(1)	0.9378(4)	4.4(1)	C(11)	0.2110(2)	0.0125(1)	0.7990(4)	4.9(1)
O(2)	−0.0576(1)	0.1334(1)	0.7497(3)	5.7(1)	C(6)	0.0577(2)	0.3328(1)	0.9169(4)	4.4(1)	C(12)	0.2817(2)	0.0669(1)	0.6419(4)	4.5(1)
C(1)	0.5012(2)	0.3546(1)	0.5291(3)	4.1(1)	C(7)	0.0365(2)	0.2917(2)	1.1539(4)	4.8(1)	C(13)	0.3959(2)	0.1050(1)	0.7668(4)	4.6(1)
C(2)	0.4453(2)	0.4259(1)	0.7401(3)	4.3(1)	C(8)	−0.0581(2)	0.2244(2)	1.1291(4)	4.9(1)	C(14)	0.4535(2)	0.1657(1)	0.6094(4)	4.4(1)
C(3)	0.2981(2)	0.4854(1)	0.7088(4)	5.0(1)	C(9)	−0.0016(2)	0.1428(1)	0.9453(4)	4.3(1)	C(15)	0.5670(2)	0.2047(2)	0.7321(4)	4.9(1)
C(4)	0.1851(2)	0.4316(1)	0.7012(4)	4.5(1)	C(10)	0.1278(2)	0.0717(1)	1.0155(4)	4.6(1)	C(16)	0.6178(2)	0.2713(2)	0.5790(5)	5.2(1)
1f														
O(1)	0.9417(1)	0.37193(8)	0.7496(2)	5.60(5)	C(7)	0.3907(1)	0.3555(1)	0.7513(3)	4.54(6)	C(14)	0.3090(1)	0.0371(1)	0.8634(3)	4.45(5)
O(2)	0.1484(1)	0.12249(8)	1.2018(2)	5.66(5)	C(8)	0.3033(1)	0.3030(1)	0.9074(3)	4.34(5)	C(15)	0.3615(1)	0.0734(1)	0.6376(3)	4.24(5)
C(1)	0.8884(1)	0.3686(1)	0.5472(3)	4.10(5)	C(9)	0.1769(1)	0.2739(1)	0.7831(3)	4.67(6)	C(16)	0.4944(1)	0.1158(1)	0.6857(3)	4.24(5)
C(2)	0.8409(1)	0.4438(1)	0.4764(3)	4.24(5)	C(10)	0.0895(1)	0.2175(1)	0.9358(3)	4.91(6)	C(17)	0.5500(1)	0.1534(1)	0.4656(3)	4.32(5)
C(3)	0.8278(1)	0.5064(1)	0.6909(3)	4.57(6)	C(11)	0.1183(1)	0.1333(1)	0.9924(2)	3.93(5)	C(18)	0.6818(1)	0.1996(1)	0.5195(3)	4.33(5)
C(4)	0.7323(1)	0.4625(1)	0.8464(3)	4.30(5)	C(12)	0.1063(1)	0.0623(1)	0.7805(3)	4.13(5)	C(19)	0.7374(1)	0.2360(1)	0.2963(3)	4.68(6)
C(5)	0.6067(1)	0.4339(1)	0.7162(3)	4.50(6)	C(13)	0.1749(1)	−0.0037(1)	0.8283(3)	4.72(6)	C(20)	0.8679(1)	0.2899(1)	0.3541(3)	4.86(6)
C(6)	0.5172(1)	0.3849(1)	0.8737(3)	4.44(6)										
1g														
O(1)	0.7694(1)	0.6071(3)	0.32105(7)	4.60(7)	C(7)	0.6332(2)	0.3282(5)	0.4920(1)	3.6(1)	C(15)	0.9206(1)	0.4726(5)	0.65976(9)	3.47(9)
O(2)	0.7152(1)	0.3616(3)	0.71043(7)	4.92(8)	C(8)	0.6182(2)	0.1462(5)	0.53551(9)	3.7(1)	C(16)	0.9836(2)	0.4621(5)	0.6186(1)	3.9(1)
C(1)	0.7085(1)	0.7474(4)	0.32052(8)	3.14(8)	C(9)	0.6919(2)	0.1506(5)	0.5848(1)	3.9(1)	C(17)	0.9716(2)	0.6648(5)	0.5764(1)	3.9(1)
C(2)	0.6222(1)	0.7013(5)	0.28302(9)	3.7(1)	C(10)	0.6795(2)	−0.0158(5)	0.6315(1)	3.8(1)	C(18)	0.8867(1)	0.6550(5)	0.5352(1)	3.7(1)
C(3)	0.5366(1)	0.7210(5)	0.3062(1)	3.6(1)	C(11)	0.7590(2)	−0.0155(5)	0.6774(1)	3.8(1)	C(19)	0.8822(1)	0.8415(5)	0.48943(9)	3.49(9)
C(4)	0.5207(1)	0.5181(5)	0.3450(1)	3.6(1)	C(12)	0.7747(1)	0.2186(4)	0.70886(8)	3.44(8)	C(20)	0.8018(1)	0.8194(5)	0.44498(9)	3.6(1)
C(5)	0.5834(1)	0.5185(5)	0.39937(9)	3.31(9)	C(13)	0.8657(2)	0.2660(6)	0.7399(1)	4.3(1)	C(21)	0.8021(2)	0.9918(5)	0.3967(1)	3.52(9)
C(6)	0.5636(1)	0.3304(4)	0.44074(9)	3.30(9)	C(14)	0.9365(2)	0.2756(5)	0.7034(1)	3.8(1)	C(22)	0.7196(1)	0.9788(4)	0.3536(1)	3.35(9)
1h														
O(1)	0.5713(1)	0.4595(2)	0.05960(5)	5.28(8)	C(8)	0.2474(2)	0.6525(3)	0.31518(7)	4.7(1)	C(17)	0.1403(2)	0.1317(3)	0.30782(7)	4.6(1)
O(2)	0.2165(2)	0.3478(2)	0.47487(5)	6.7(1)	C(9)	0.1393(2)	0.6415(3)	0.35068(7)	4.6(1)	C(18)	0.2631(2)	0.1442(3)	0.27829(7)	4.6(1)
C(1)	0.4503(2)	0.4747(3)	0.05487(6)	4.0(1)	C(10)	0.1920(2)	0.6505(3)	0.40106(7)	4.7(1)	C(19)	0.2318(2)	0.1445(3)	0.22603(7)	4.6(1)
C(2)	0.3863(2)	0.6427(3)	0.05460(7)	5.2(1)	C(11)	0.0858(2)	0.6292(3)	0.43777(7)	4.8(1)	C(20)	0.3539(2)	0.1449(3)	0.19614(7)	4.6(1)
C(3)	0.2872(2)	0.6687(3)	0.09274(7)	5.2(1)	C(12)	0.0202(2)	0.4599(3)	0.43734(7)	4.6(1)	C(21)	0.3227(2)	0.1548(3)	0.14411(7)	4.4(1)
C(4)	0.3494(2)	0.6532(3)	0.14193(7)	4.6(1)	C(13)	0.1121(2)	0.3206(3)	0.45288(7)	4.6(1)	C(22)	0.4468(2)	0.1488(3)	0.11454(7)	4.8(1)
C(5)	0.2463(2)	0.6595(3)	0.17924(7)	4.7(1)	C(14)	0.0680(2)	0.1480(3)	0.44136(7)	5.2(1)	C(23)	0.4198(2)	0.1632(3)	0.06188(7)	5.0(1)
C(6)	0.3021(2)	0.6524(3)	0.22880(7)	4.6(1)	C(15)	0.0453(2)	0.1153(3)	0.38885(7)	4.9(1)	C(24)	0.3601(2)	0.3272(3)	0.04651(7)	4.7(1)
C(7)	0.1951(2)	0.6488(3)	0.26504(7)	4.6(1)	C(16)	0.1691(2)	0.1420(3)	0.36027(7)	4.5(1)					
1i (n)														
O(1)	0.0372(2)	0.2481(3)	0.29543(4)	5.71(7)	C(5)	0.2013(2)	0.4371(3)	0.44818(6)	4.20(8)	C(10)	0.5038(2)	−0.1427(3)	0.63723(6)	4.49(8)
C(1)	−0.0775(2)	0.3877(4)	0.29593(5)	3.96(8)	C(6)	0.1890(2)	0.2469(3)	0.48624(6)	4.28(8)	C(11)	0.3720(2)	−0.1369(3)	0.67020(6)	4.11(8)
C(2)	−0.0597(2)	0.6107(3)	0.32657(6)	4.17(8)	C(7)	0.3358(2)	0.2504(3)	0.52576(6)	4.37(8)	C(12)	0.3900(2)	−0.3349(3)	0.70788(6)	4.26(8)
C(3)	0.0845(2)	0.6085(3)	0.36693(6)	4.23(8)	C(8)	0.3346(2)	0.0555(3)	0.56358(6)	4.30(8)	C(13)	0.2406(2)	−0.3466(4)	0.73534(6)	4.58(8)
C(4)	0.0628(2)	0.4295(3)	0.40631(6)	4.32(8)	C(9)	0.4898(2)	0.0598(3)	0.60075(6)	4.56(9)					
1i (pl)														
O(1)	−0.3748(2)	0.30972(4)	−0.0306(1)	5.86(6)	C(5)	0.3812(2)	0.40754(4)	0.2553(2)	3.85(6)	C(10)	0.8238(2)	0.61722(4)	0.2722(2)	3.71(5)
C(1)	−0.1612(2)	0.30106(4)	0.0179(2)	3.41(5)	C(6)	0.3593(2)	0.46083(4)	0.2376(2)	3.84(6)	C(11)	1.0749(2)	0.64008(5)	0.3049(2)	3.99(6)
C(2)	−0.0614(2)	0.29980(4)	0.2039(2)	3.63(5)	C(7)	0.6030(3)	0.48595(5)	0.2651(2)	4.05(6)	C(12)	1.0770(3)	0.69373(5)	0.2863(2)	4.18(6)
C(3)	0.1716(2)	0.32821(4)	0.2561(2)	3.51(5)	C(8)	0.5879(2)	0.53942(4)	0.2549(2)	3.82(6)	C(13)	0.9931(2)	0.71097(4)	0.1073(2)	3.54(5)
C(4)	0.1414(2)	0.38092(4)	0.2236(2)	3.58(5)	C(9)	0.8347(2)	0.56369(4)	0.2847(2)	3.97(6)					
1j														
O(1)	0.33611(4)	0.2861(1)	−0.04200(8)	5.60(4)	C(3)	0.40083(6)	0.0930(2)	0.2570(1)	5.45(5)	C(6)	0.41879(6)	0.6042(2)	0.1091(1)	4.82(4)
C(1)	0.33107(5)	0.2755(1)	0.0780(1)	4.56(4)	C(4)	0.46781(6)	0.0984(2)	0.1965(1)	4.97(5)	C(7)	0.34069(6)	0.5918(2)	0.1060(1)	5.39(5)
C(2)	0.33593(6)	0.1095(2)	0.1499(2)	5.72(5)	C(5)	0.46135(5)	0.6003(1)	0.2509(1)	4.55(4)	C(8)	0.31715(6)	0.4275(2)	0.1597(1)	5.05(5)
4d														
O(1)	0.2754(2)	0.6250(1)	0.1886(2)	5.43(4)	C(5)	−0.0174(2)	0.1724(2)	0.2314(2)	4.48(6)	C(11)	0.5963(2)	0.1625(3)	0.3179(3)	4.92(7)
O(2)	0.4320(1)	0.1962(1)	0.5248(1)	5.19(4)	C(6)	0.0836(2)	0.1923(3)	0.4031(2)	4.93(7)	C(12)	0.5515(2)	0.2442(3)	0.2152(3)	4.67(7)
C(1)	0.2940(2)	0.4588(2)	0.0876(2)	3.77(5)	C(7)	0.1205(2)	0.0443(3)	0.3947(3)	5.19(7)	C(13)	0.4241(2)	0.3183(2)	0.2297(2)	3.68(5)
C(2)	0.1089(2)	0.3720(2)	0.0843(2)	3.88(5)	C(8)	0.2132(2)	−0.0168(2)	0.2948(3)	4.63(6)	C(14)	0.3902(2)	0.3978(2)	0.1249(2)	3.71(5)
C(3)	0.1023(2)	0.4292(2)	0.2571(2)	4.38(6)	C(9)	0.3749(2)	0.0835(2)	0.3781(2)	3.80(5)	C(15)	0.3363(3)	0.2969(2)	−0.0726(2)	4.81(6)
C(4)	−0.0355(2)	0.3273(2)	0.2422(3)	4.80(6)	C(10)	0.4658(2)	0.0318(2)	0.2749(3)	4.71(6)	C(16)	0.2359(2)	0.4009(3)	−0.0958(3)	5.06(7)
4j														
O(1)	0.9452(1)	0.1610(1)	0.4673(2)	6.82(5)	C(5)	0.6114(2)	0.1572(2)	0.2522(2)	5.33(6)	C(11)	0.7782(2)	0.3511(2)	0.9636(2)	6.74(8)
O(2)	0.2865(1)	0.2086(1)	0.6473(2)	5.18(4)	C(6)	0.6821(2)	0.0889(1)	0.4104(2)	4.81(6)	C(12)	0.5957(2)	0.3203(2)	0.8822(2)	5.88(7)
C(1)	0.2327(2)	0.3307(1)	0.3947(2)	5.17(6)	C(7)	0.8597(2)	0.1176(1)	0.5328(2)	4.78(6)	C(13)	0.5049(2)	0.3338(1)	0.6819(2)	4.59(5)
C(2)	0.3134(2)	0.2986(2)	0.2697(2)	5.51(6)	C(8)	0.9294(2)	0.0888(2)	0.7246(3)	5.89(7)	C(14)	0.3213(2)	0.3162(1)	0.6005(2)	4.50(5)
C(3)	0.3229(2)	0.1666(2)	0.2275(2)	5.09(6)	C(9)	0.8501(2)	0.1517(2)	0.8399(2)	5.60(7)	C(15)	0.2407(2)	0.4271(2)	0.6432(3)	7.23(9)
C(4)	0.4292(2)	0.1284(2)	0.1322(2)	6.20(7)	C(10)	0.8623(2)	0.2849(2)	0.8565(2)	5.66(6)	C(16)	0.2103(2)	0.4593(2)	0.4568(4)	7.6(1)
4′j														
O(1)	−0.0884(1)	0.2892(1)	0.30791(8)	5.36(7)	C(5)	−0.0607(2)	0.1722(2)	0.3299(1)	4.14(8)	C(11)	0.5304(2)	0.2519(2)	0.5083(1)	5.1(1)
O(2)	0.6123(1)	−0.0192(1)	0.32334(8)	4.48(6)	C(6)	−0.0423(2)	0.1327(2)	0.4173(1)	4.53(9)	C(12)	0.5334(2)	0.1448(2)	0.4427(1)	4.20(8)
C(1)	0.3623(2)	0.0647(2)	0.2504(1)	3.62(7)	C(7)	−0.0245(2)	0.2484(2)	0.4783(1)	5.2(1)	C(13)	0.5436(2)	0.2010(2)	0.3595(1)	3.86(7)
C(2)	0.2335(2)	0.0795(2)	0.2927(1)	3.88(7)	C(8)	0.1143(2)	0.3324(2)	0.4825(1)	5.0(1)	C(14)	0.5245(2)	0.0945(2)	0.2922(1)	3.55(7)

Table 11 (Continued)

atom	*x*	*y*	*z*	B_{eq}	atom	*x*	*y*	*z*	B_{eq}	atom	*x*	*y*	*z*	B_{eq}
4′1j (Continued)														
C(3)	0.0885(2)	0.0806(2)	0.2316(1)	4.63(9)	C(9)	0.2555(2)	0.2536(2)	0.5076(1)	4.73(9)	C(15)	0.5470(2)	0.1525(2)	0.2102(1)	4.55(9)
C(4)	−0.0463(2)	0.0620(2)	0.2694(1)	5.1(1)	C(10)	0.3905(2)	0.3345(2)	0.4981(1)	5.0(1)	C(16)	0.3805(2)	0.1689(2)	0.1850(1)	4.79(9)
5f														
O(1)	0.1954(3)	0.2068(2)	0.2162(3)	5.4(2)	C(7)	0.0978(5)	0.7373(4)	0.5281(5)	9.2(3)	C(14)	0.1899(3)	0.6011(2)	−0.0027(3)	4.5(2)
O(2)	−0.0670(2)	0.8833(2)	0.0613(2)	5.8(1)	C(8)[b]	0.1380(6)	0.7573(4)	0.3989(6)	7.0(4)	C(15)	0.3040(3)	0.4744(3)	0.0194(3)	4.7(2)
C(1)	0.3594(3)	0.1763(3)	0.2663(3)	4.7(2)	C(8a)[c]	0.028(2)	0.804(2)	0.390(2)	7.0(5)	C(16)	0.2324(3)	0.3787(3)	−0.0035(3)	4.6(2)
C(2)	0.3919(4)	0.2185(3)	0.4224(4)	5.9(2)	C(9)	0.0910(5)	0.8915(4)	0.3632(4)	7.8(3)	C(17)	0.3506(3)	0.2517(3)	0.0160(3)	4.6(2)
C(3)	0.3196(4)	0.3519(3)	0.4377(3)	6.0(2)	C(10)	0.1539(4)	0.8993(3)	0.2404(4)	6.2(2)	C(18)	0.4419(3)	0.2159(2)	0.1725(3)	4.3(2)
C(4)	0.3445(4)	0.3961(4)	0.5942(4)	7.2(3)	C(11)	0.0698(4)	0.8674(2)	0.0922(3)	4.6(2)	C(19)	0.5648(4)	0.0888(3)	0.1923(4)	6.1(2)
C(5)	0.3041(5)	0.5306(4)	0.6050(4)	7.5(3)	C(12)	0.1620(3)	0.8201(3)	−0.0161(3)	5.1(2)	C(20)	0.4572(4)	0.0463(3)	0.2449(4)	6.6(2)
C(6)	0.1358(5)	0.6032(4)	0.5471(4)	8.0(3)	C(13)	0.2706(3)	0.6910(3)	0.0131(3)	4.9(2)					

[a] $B_{eq} = (8/3)\pi^2\sum\sum U_{ij}a_i^*a_j^*(\mathbf{a}_i\cdot\mathbf{a}_j)$. [b] Site occupancy 0.77. [c] Site occupancy 0.23.

macrocyclic (≥16-membered-ring) diketones that leads to the different photoproduct distributions noted above.

This general picture, whereby the conformational properties of the 16-membered (and larger) rings are likened to those of acyclic compounds, is in agreement with the results of the photolysis of conformationally flexible noncyclic ketones, where the rate of rotation around carbon−carbon bonds in the triplet biradical intermediate is known to be greater than that of cleavage or cyclization.[18,60] In such cases, as in the case of the 16-membered-ring diketone **1d**, cleavage is the major course of reaction, and *trans*-cyclobutanols are generally formed in preference to *cis*. As can be seen from Table 1, the solution phase photoproduct ratios for the 18- to 26-membered-ring diketones **1e**−**1i** also follow this trend. Similarly, in the monoketone homologous series, the fraction of cleavage photoproducts increases markedly with ring size, going from 8% in cycloundecanone to 58% in cyclohexadecanone.[7] At the same time, the proportion of *cis*-cyclobutanol decreases from 40% to 13%.

Concluding Remarks and Summary. In many respects, the results reported in this paper resemble the classic studies of Schmidt and co-workers on the photochemistry of cinnamic acid and its derivatives in the crystalline state[61]—studies that were instrumental in laying the groundwork for and stimulating interest in the field of solid state organic chemistry. In both Schmidt's work and ours, distance and geometric requirements for photoreaction have been established, and the structure and stereochemistry of the products have been shown to be simply and directly related to the molecular and crystal structure of the reactants. In the case of the cinnamic acids, the reaction studied was bimolecular ([2 + 2] photocycloaddition), whereas the diametric diketones react unimolecularly in the crystalline state. Nevertheless, similar conclusions were reached: reactions occurring through certain geometries lead to products whose structure and stereochemistry are those predicted by least motion pathways originating from the molecules as they are arranged in the bulk crystal. For the diketones, carbonyl oxygen−γ-hydrogen contacts averaging 2.74 ± 0.04 Å, along with values of the angular parameters ω, Δ, and θ of 53 ± 5°, 83 ± 4°, and 115 ± 2°, respectively, are identified as leading to abstraction.[62] Following abstraction, the 1,4-hydroxy biradical intermediates cyclize over carbon−carbon distances of 3.1−3.2 Å with "retention of configuration" at the radical terminii such that *trans*-fused cyclobutanol derivatives are formed in some cases and *cis*-fused cyclobutanols are formed in others depending on the conformation adopted by the diketone in the solid state.

These geometric criteria represent a substantial first step toward making it possible to "crystal engineer" the intramolecular hydrogen abstraction reactions of carbonyl compounds, that is to be able to *design* molecular crystals that will undergo a desired reaction of this type. Because such reactions are unimolecular in nature and depend on conformation, and because conformation can now be predicted quite accurately by using empirical force field methods, and because the lowest energy conformation calculated by such methods is very often the same basic conformation adopted by the molecule in the crystalline state, the probable success or failure of a hypothetical hydrogen atom abstraction reaction in the solid state can now be evaluated in a relatively straightforward manner. As the instructive case of 1,6-cyclodecanedione (**1a**) reminds us, however, (a) the lowest energy molecular conformation is not always found in the crystal and (b) a favorable solid state hydrogen atom abstraction geometry alone does not guarantee observable photoproduct formation—the ongoing reactions of the 1,4-hydroxy biradical must be competitive with reverse hydrogen atom transfer as well. When this is the case, as it is for 10 of the 11 crystalline materials investigated in this study, the results provide a compelling demonstration of the ability of the Crystal Structure−Reactivity Correlation Method to clarify the geometric requirements of a basic solid state photochemical reaction—results that have strong implications for the corresponding solution phase process as well.

Experimental Section

X-ray Crystallographic Analyses. Crystallographic data are summarized in Table 3. The data were processed[63] and corrected for Lorentz and polarization effects and absorption (empirical, based on azimuthal scans for three reflections).

The structures were all solved by direct methods. The non-hydrogen atoms were refined with anisotropic thermal parameters. Hydrogen atoms were visible on difference maps and were refined or included in idealized positions (C−H = 0.98 or 0.99 Å, *B*(H) = 1.2*B*(parent atom), see Table 3). The ring atom C(8) in compound **5f** was modeled as 2-fold disordered, and the site occupancy factors were adjusted as the refinement progressed to give nearly equal equivalent isotropic thermal parameters for the two component atoms (C(8) and C(8a)). Neutral atom scattering factors and anomalous dispersion corrections were taken from the *International Tables for X-Ray Crystallography*.[64]

Final atomic coordinates and equivalent isotropic thermal parameters for the non-hydrogen atoms are given in Table 11. Hydrogen atom coordinates, anisotropic thermal parameters, bond lengths, bond angles, torsion angles, intermolecular contacts, and least-squares planes for all 13 structures are included as supporting information.

---

(60) Scaiano, J. C.; Lissi, E. A.; Encina, M. V. *Rev. Chem. Intermed.* **1978**, *2*, 139.

(61) Schmidt, G. M. J. *Pure Appl. Chem.* **1971**, *27*, 647.

(62) It should be emphasized that these are *ground state* geometric parameters and that theoretical treatments such as those of Dorigo et al. (Dorigo, A. E.; McCarrick, M. A.; Loncharich, R. J.; Houk, K. N. *J. Am. Chem. Soc.* **1990**, *112*, 7508) and Sauers *et al.*[40] give a more accurate picture of the hydrogen atom abstraction geometry at the transition state.

(63) TEXSAN: Crystal Structure Analysis Package (Version 5.1); Molecular Structure Corporation: The Woodlands, TX, 1985.

(64) *International Tables for X-Ray Crystallography*; Kynoch Press: Birmingham, England, 1974; Vol. IV, pp 99−102 and 149.

Acknowledgment. We thank the donors of the Petroleum Research Fund, administered by the American Chemical Society, for partial support of this research. Financial support by the Natural Sciences and Engineering Research Council of Canada is also gratefully acknowledged. This project has benefitted greatly from the assistance of the following individuals, whom we thank: Professor Larry Weiler (help with the MM2 calculations), Professor Colin Fyfe (solid state NMR studies), and Professor Ron Sauers (calculations on the feasibility of hydrogen abstraction in 1,6-cyclodecanedione).

Supporting Information Available: Experimental details of diketone preparation, photolysis procedures, separation and characterization of photoproducts, molecular mechanics calculations, hydrogen atom coordinates, anisotropic thermal parameters, bond lengths, bond angles, torsion angles, intermolecular contacts, and least-squares planes for the 13 X-ray crystal structures (209 pages). Ordering information is given on any current masthead page.

JA953420A